MIST COOLING OF HOT METALLIC SURFACES

by

K. VIDYA

DEPARTMENT OF MATERIALS AND METALLURGICAL ENGINEERING
INDIAN INSTITUTE OF TECHNOLOGY KANPUR
AUGUST, 1994

MME - 1994 - M - VID - MIS

CERTIFICATE

It is certified that the work contained in the thesis entitled *"Mist Cooling of Hot Metallic Surfaces"*, by K. Vidya, has been carried out under my supervision and that this work has not been submitted elsewhere for a degree.

Dr. S. C. Koria

Professor

Department of Materials and Metallurgical Engineering

Indian Institute of Technology Kanpur

August 1994

ABSTRACT

Design of mist and water spray nozzles and their heat extraction capability is studied via heat transfer and quenching mechanisms.

To appreciate the nozzle design, variation of pressure with flow rate for single phase flow, effect of water flow rate on the variation of air pressure with air flow rate in two phase flow, two phase flow structure and the water flux distribution in the mist are studied. Some of the experiments are considered for the water spray nozzle also.

The performance of the nozzles are evaluated by the heat transfer measurements for steel, copper and brass samples. Quenching is carried out for the steel samples, and the microstructure of the specimens are observed under optical microscope.

It is found that the pressure drop for the single phase flow for mist nozzle always greater than water spray nozzle. The structure of the two phase flow depends on the combination of water and air flow rate.

Heat transfer studies reveal that the mechanisms of the transfer is similar to pool boiling. Heat transfer coefficient increases with decrease in surface temperature. At higher temperature (600–800°C) there is no effect of water flux hitting hot surface, initial temperature and the carbon content of steel. Thermophysical properties affect the heat transfer coefficients. At any surface temperature, $h_{copper} > h_{brass} > h_{steel}$. It is found that h_{mist} is grater than $h_{water\ spray}$ for some water flow rate.

Mist cooling has an application in the area of secondary cooling in continuous casting, rolling and in heat treatment.

TABLE OF CONTENTS

LIST OF FIGURES

LIST OF TABLES

LIST OF SYMBOL

A	Region of partial water jet
B	Region of coarse mist
C	Region of mist
C_p	Specific heat
D	Region of pulsation
h	Heat transfer coefficient
k	Thermal conductivity
P_a	Pressure (pressure drop) for gas alone
P_w	Pressure (pressure drop) for water alone
P_{aw}	Air pressure in presence of water
q	Heat flux
$\dot{q}_w$	Water flux hitting the hot surface
Q_a	Volume flow rate of air
Q_w	Volume flow rate of water
t	Time
T	Temperature
T_s	Surface temperature
T_i	Initial temperature
x_o	Spray distance
x	Co-ordinates
ρ	Density

CHAPTER 1

INTRODUCTION

The technique of cooling hot metallic surfaces by mist has many technical applications in secondary cooling in continuous casting, heat treatment and rolling. Mist cooling is widely used because of its uniformity in cooling, greater cooling rate and less nozzle clogging. The water droplets are finer and more distributed in the air jet.Due to finer droplets, the mist jet possesses larger kinetic energy.

Secondary cooling during continuous casting, decides the final quality of the continuous cast product. Type of cooling influences the defect formation by generating tensile stresses, by altering the strand temperature and hence, the mechanical properties, by influencing the precipitation of second phases which lower steel ductility and by slightly influencing the solidification rate. In continuous casting, the slabs are more prone to defects as compared to billets. Because of their large rectangular shape, it may bulge under the influence of ferrostatic pressure. The mist cooling can give uniform cooling through out the slab surface.

Spray cooling of a high temperature steel surface involves boiling heat transfer coupled with the dynamics of the approaching water droplets. The ability of approaching droplets to penetrate the vapour boundary layer is influenced by their momentum, which in turn is related to the droplet size and velocity. Once the boundary layer is penetrated, the wetting action of water accelerates the degree of heat extraction. The above mechanism of heat transfer is considerably influenced by mist spray. In air-atomized method, violent turbulence of atomized water flow on the

surface being cooled facilitates uniform contact of water droplets with hot surface, and the atomised water flow impinging with a high speed against hot surface being cooled makes the vapour film over the surface unstable and facilitates heat transfer.

Present investigation involves the characterization of mist and water spray nozzles and comparison of their heat extraction capability. Chapter 2 deals with the review of the earlier work done. In chapter 3, experimental set-up and procedure are given and these results are discussed in chapter 4. In chapter 5, the conclusions based on the present results are given. Chapter 6 gives the suggestions for the further work.

CHAPTER 2

LITERATURE REVIEW

The process of water cooling hot metal surface has many important technical aspects in the liquid and solid metal processing area. For example in continuous casting, a partially solidified bloom, billet or slab is cooled by number of water sprays in the secondary cooling zone in order to get a completely solidified product. Fig.2.1 depicts the schematic representation of the process of cooling in continuous casting. In this high pressure, water sprays are used and the sprays are directed from all sides on the bloom, billet or slab. The vertical height of the secondary cooling zone is generally of the order of fifty times the maximum casting direction. Nearly ninety percent of the heat is extracted from this zone [1].

Similarly, the hot rolled or the continuously cast billet are cooled to a given temperature on the cooling beds and delivered to the subsequent process [2]. Fig.2.2 shows the schematic view of the cooling bed which consists of entry, cooling and delivery zone.

In heat treatment, water is one of the widely used quenching medium of hot rolled metallic surfaces.

2.1 COOLING REQUIREMENTS

In order to increase the thermal efficiency and the cooling homogeneity and consequently to improve the metallurgical quality of the cast product [1], the cooling water

    1) must be sprayed very finely.

POURING

COOLING WATER

LIQUID
POOL

HOLLOW
COPPER
MOULD

Z

WATER SPRAY

SOLID
STEEL

SECONDARY
COOLING
ZONE

MUSHY
ZONE

ROLLS
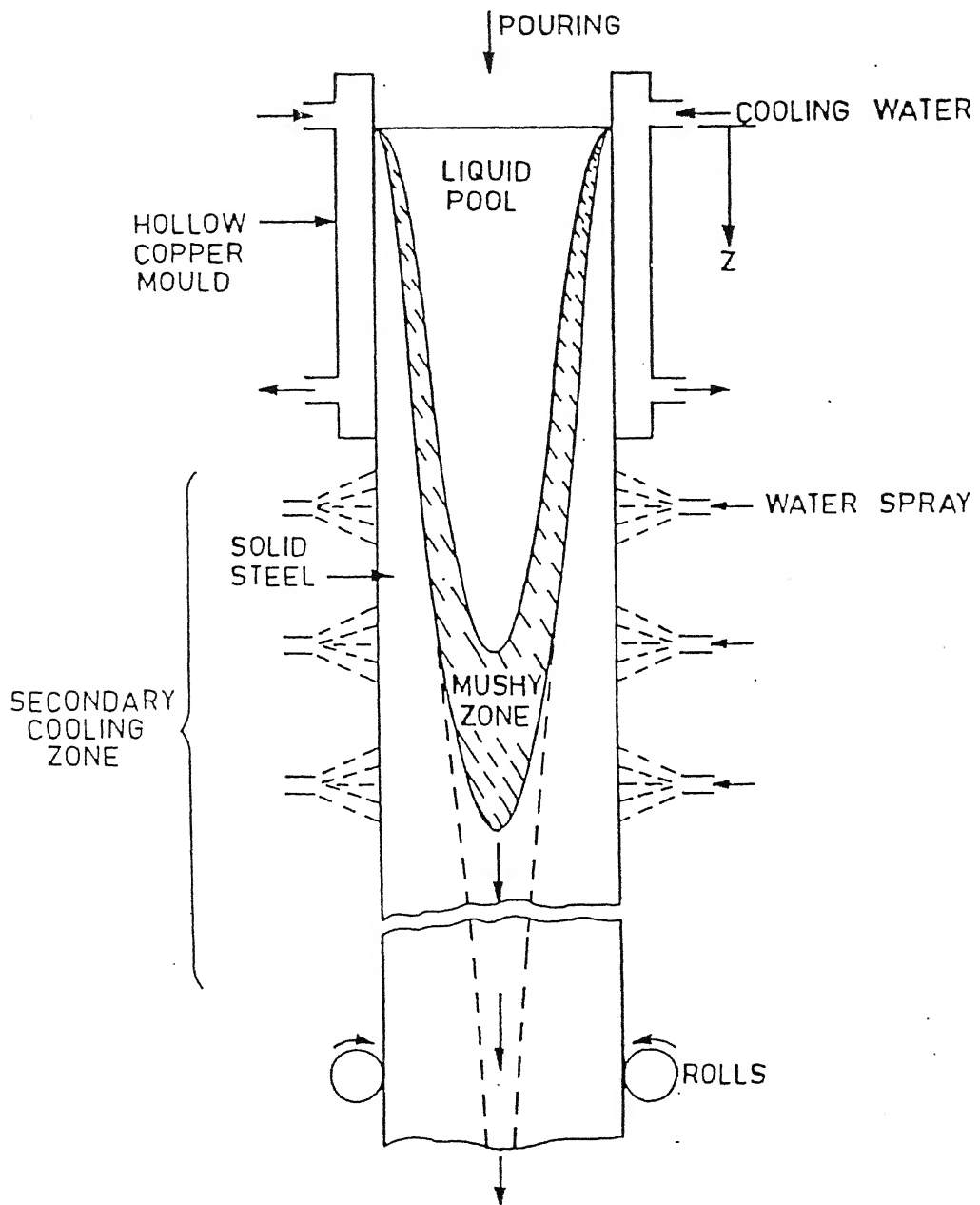
Fig. 2.1 Secondary cooling in continuous casting process.
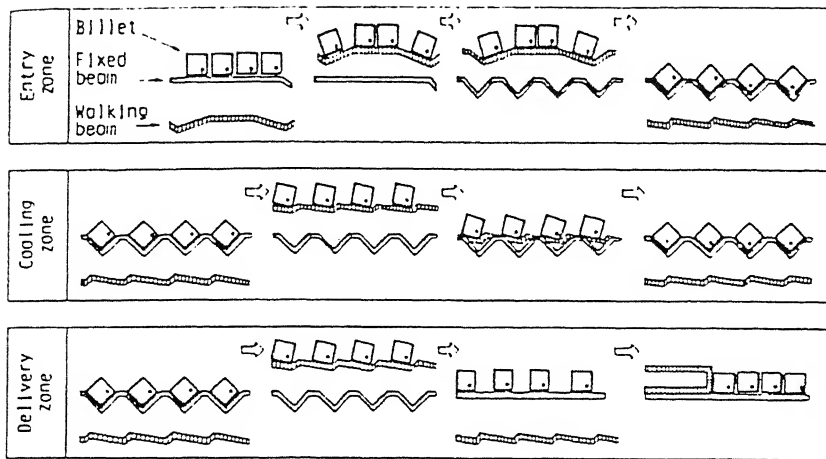
Fig. 2.2 Schematic illustration of billet rotation process on the walking beam type cooling bed.
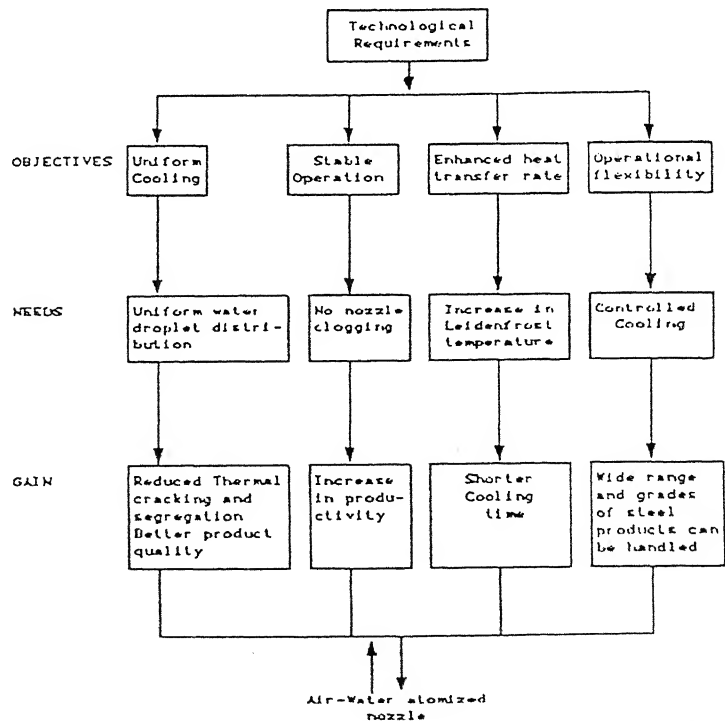
Fig. 2.3 Process technological incentives for developing mist nozzle.

2) the water droplets must have high speed.

3) the impact surface of the hot material must be large.

4) the calcification that hinders the heat exchange must be reduced.

The use of air atomised mist nozzle fulfills the above requirements and ensures a high quality of the cast product. It is important to atomize a water stream uniformly into a stable mist stream. This can be easily achieved by the increase of the ratio of air - water mass flow rate (Q_a / Q_w) or the increase of air flow rate. Expanding the variable range of water flow rate (Q_w) satisfies the above requirement. The range of Q_w in mist cooling is subjected to the following constraints.

Lower limit :

1) uniform distribution of water zone.

2) stability of water atomization (mist stream) measure against pulsation.

Upper limit :

1) water and air supply capability.

2) maximum atomization capability of air on water.

The condition of mist stream is strongly affected by the construction of the nozzle and the nozzle orifice diameter, flow rate and the pressure of both water and air. The technique of cooling the hot steel surface by mist has many important technical applications like - heat treatment of steel secondary cooling of continuous casting etc. This is because air - water mist provides more uniform cooling.

2.2 COMPARISON OF MIST COOLING WITH SPRAY COOLING

In mist cooling, air has a double role to play, mechanically to

divide the water into fine droplets in the form of mist and to impart the considerable kinetic energy to the droplets. The atomization characteristics depend on the pressure and the consumption of water. The cooling capacity of the mist having very low velocity of air is hardly influenced by the nozzle design [3]. When velocity increases, the momentum of water droplets increases and at the same time the mist, impinging on the specimen, flows violently on the specimen surface. When the velocity of the air is low then the air flow has a role only in the water atomization. Process technological incentives for developing mist nozzle are given in Fig.2.3 [4].

2.2.1 Cooling Efficiency

Due to the increase in water flux for the same water flow rate, this mist jet has high kinetic energy and large quantity of the atomized water comes into the contact with the metal. Since the water droplets are fine and numerous, the area of heat exchange between water and hot surface is increased. Air water mist nozzle produces droplets of 20 - 60 μm in size whereas those in water spray are 200 - 600 μm in size [5].

2.2.2 Homogeneity and Uniformity of Cooling

The cooling is more homogeneous and less severe locally than that obtained with a water spray. The full cone jet ensures a uniform and continuous distribution of water. Therefore this method reduces thermal shock and risk of cracking.

2.2.3 Flexibility of Operation

The maximum to minimum consumption of water is much larger compared to water spray. For air - water mist nozzle, it is obtained with in a ratio of 8 to 1 [6].But for water spray, it is limited to about 3 to 1

at the best [6,7]. To get the proper mist, either we can modify the consumption of water or air or both simultaneously.

2.2.4   Nozzle Clogging

Nozzle clogging at high pressure is estimated due to the atomization of water at very large nozzle diameters. For the air-atomised mist, smaller nozzle diameters can be used to decrease nozzle clogging is reduced.

2.3 TYPES OF MIST NOZZLE

The typical requirements of for the mist nozzle are :

1) atomization of cooling water into a fine mist.

2) wide range discharge of mist stream - reduction in number of nozzle discharged.

3) increase in size of the nozzle outlet - in nozzle clogging and increase in the discharged water volume range.

4) water flow rates of the secondary cooling must be controllable within a ratio of 1 to 8 (maximum to minimum water flow rate).

The atomization of water is brought about by the impact of air jet and the atomizer behaves like two separate injectors overlapping each other. This mixing can take place either inside or outside the nozzle and this mainly depends on the design of the nozzle.

The whole secondary cooling of MITSUBISHI steel MFG continuous caster is equipped with mist nozzle [6]. Fig.2.4 shows the operating mode and the shape, the angle and the thickness of the atomized water jet depend on the nozzle tip. Fig.2.5 shows the atomizer used in FCB atomization
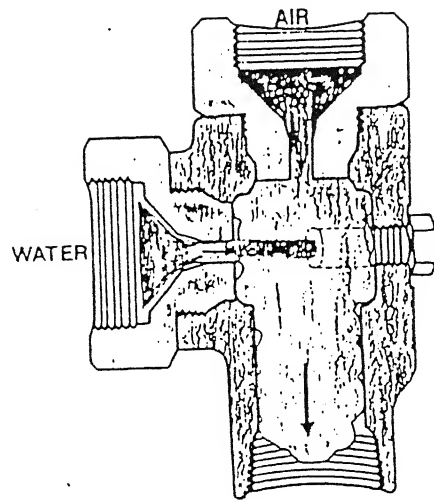
Fig. 2.4 Operation mode of an air-water spray nozzle.
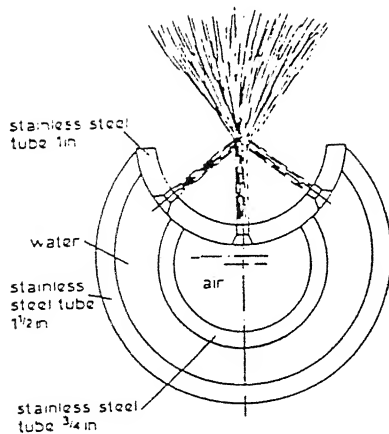
Fig. 2.5 Section of an atomization
distributor.
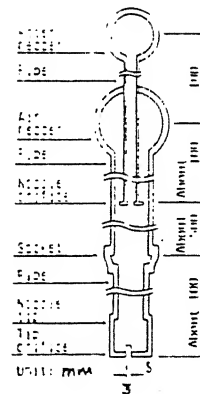
Fig. 2.6 Schematic diagram of a newly
developed practical mist nozzle.

distributors designed at CEREP at Usinor Derkirk [8]. The practical small mist is shown in Fig.2.6. The premixed method that uses compressed air was adopted to decrease the size of the nozzle and the pipeline [3]. In spite of large turn - down range, the mist nozzle which are used in the industry is given in Fig.2.7.

2.4 SPRAY CHARACTERIZATION OF THE NOZZLE [9]

'Controlled' spray cooling in continuous casting provides a real incentive for understanding the effect of spray parameters on the rate of heat extraction. There are number of primary parameters which influences the rate of heat extraction obtainable with a water spray system viz. water flux, mean drop size, drop velocity, angle of impingement and wetting effects. The uniformity of heat extraction is strongly dependent on the distribution of droplet flux within the spray pattern

The influence of water pressure, nozzle design and spray distance on the spray profile are given in Fig.2.8 to Fig.2.10.

2.5 MECHANISM OF COOLING

Spray cooling of hot metallic surface by water, shown in Fig.(2.11) involves boiling heat transfer coupled with dynamics of the approaching water droplet. The ability of the approaching water droplets to penetrate the vapour boundary layer is influenced by their momentum, which in turn is related to droplet size and approaching velocity [10]. Pederson [11] carried out a fundamental study. He employed droplet diameter 0.2 - 0.4 mm, droplet approach velocity of 2.5 - 10 m s^{-1}. The surface temperature is ranged up to 1000 $^{\circ}$C. Photograph of the impingement process
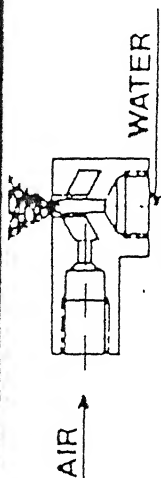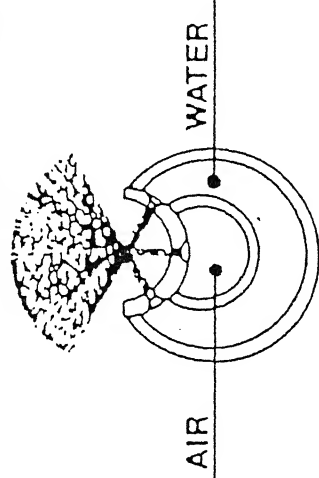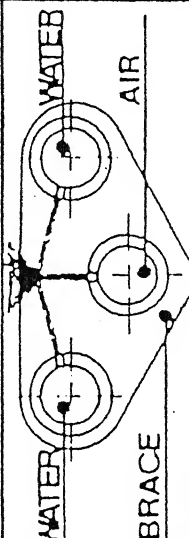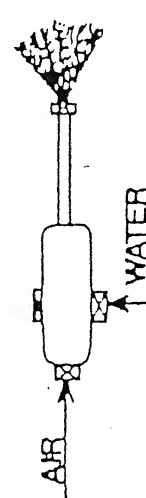
ACHIEVEMENTS	YEAR	SPRAY-NOZZLE TYPE	AIR/WATER Nm³/m³
FIRST TESTS OF ATOMIZING ON BLOOM CONTINUOUS CASTER AT DENAIN.	1972 – 1973	WATER / AIR	143
-TESTS ON No.11 SLAB CONTINUOUS CASTER AT USINOR DUNKIRK.	1974		39
-TESTS ON CENTRIFUGAL BILLET CONTINUOUS CASTER AT DECAZEVILLE. -START UP OF BILLET AND BLOOM C.C AT SIDERPERU (PERU). -TESTS ON SLAB C.C AT CLABECQ (BELGIUM).	1975 / 1977 / 1979	WATER / AIR	34
-FITTING NEW ATOMIZING NOZZLES TO BLOOM C.C AT DENAIN. -START UP OF BLOOM C.C AT USINOR NEUVES MAISONS.	1979 – 1980 / 1981	WATER / AIR / BRACE	34
-TESTS ON BLOOM C.C AT DENAIN. -FITTING BELOW THE MOLD ON BLOOM C.C AT USINOR NEUVES MAISONS. -START UP OF THE SLAB C.C AT SOLMER. -START UP OF THE BLOOM C.C AT MSM -START UP OF THE BILLET C.C AT UNM -START UP OF THE BLOOM C.C AT SAFE	1982 / 1983 / 1984 / 1984 / 1985 / 1986	WATER / AIR	25

Fig. 2.7 Various types of nozzle design used in industry.
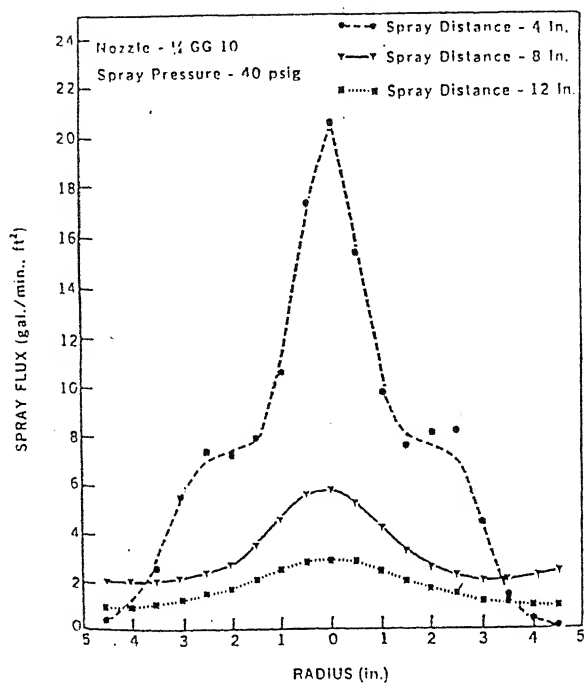
Fig. 2.8 Variation of spray water flux as a function of spray distance.
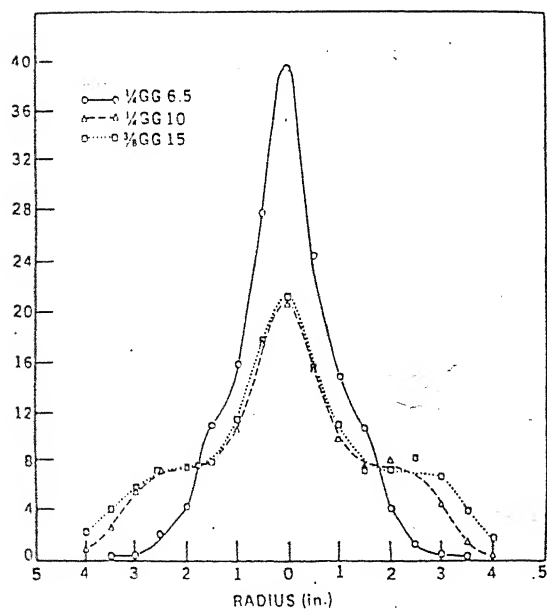
Fig. 2.9 Variation of spray water flux as function of nozzle design.
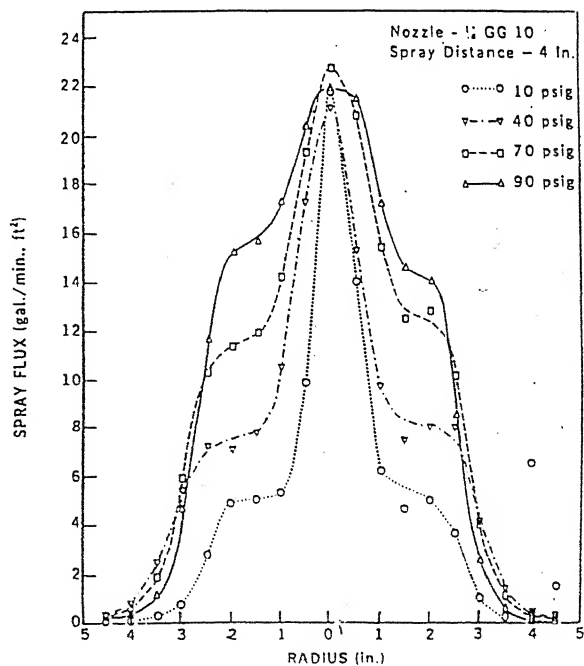
Fig. 2.10 Variation of spray water flu as function of spray pressur

showed that even the small droplets broke up upon impingement at moderate approach velocity. At low surface temperature, steam formation is slow and hence the droplets tend to 'wet' the steel surface. This results into a good contact between surface and water and enhances heat exchange at the surface significantly. However at higher surface temperature, drops would not wet the surface with the consequence of that surface heat transfer decreases. Fig (2.12) demonstrates this effect. In the non wetting regime, heat transfer per droplet was found to increase significantly with the approach velocity of droplet.

F. Akao et. al. [12] has studied the deformation behaviour of a liquid droplet impinging into a hot metal surface. Water, ethanol and acetic acid are used at 400 ^{o}C to study the individual droplet behaviour of the spray. Fig. (2.13) gives the photographs of the boiling droplets. The similar kind of work was reported by Savic and Boult [13] and Wachtars and Westerling [14].

2.5.1 Fundamental Correlation for Heat Transfer by Spray Water Cooling

Cooling of hot metallic surface by water involves boiling heat transfer coupled with the dynamics of the approaching water droplets. The ability of the approaching water droplets to penetrate the vapour boundary layer is influenced by their momentum, which in turn is related to the droplet size and approaching velocity [10]. Once the boundary layer is penetrated it is likely that the wetting action and the angle of impingement of the droplet will have an effect on the degree of heat extraction.

A simple system consisting of a heating surface submerged in a pool of water at saturation temperature without external agitation is called pool boiling. There are six regimes of boiling associated with the
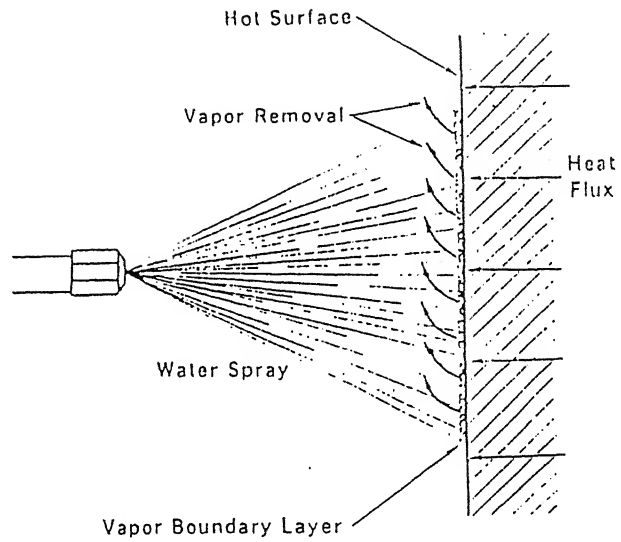
Fig. 2.11 Spray cooling of high temperature surface.

-0.23 ms	0.11 ms	0.44 ms	0.77 ms
1.44 ms	2.11 ms	2.44 ms	3.11 ms
4.44 ms	6.44 ms	7.44 ms	8.44 ms
10.4 ms	12.1 ms	12.8 ms	14.7 ms
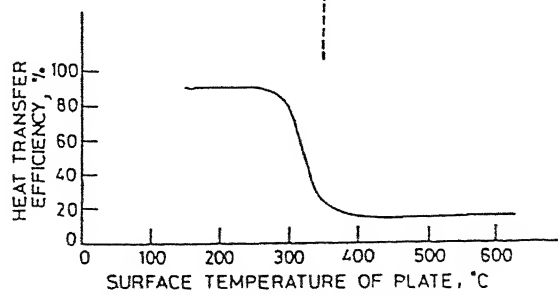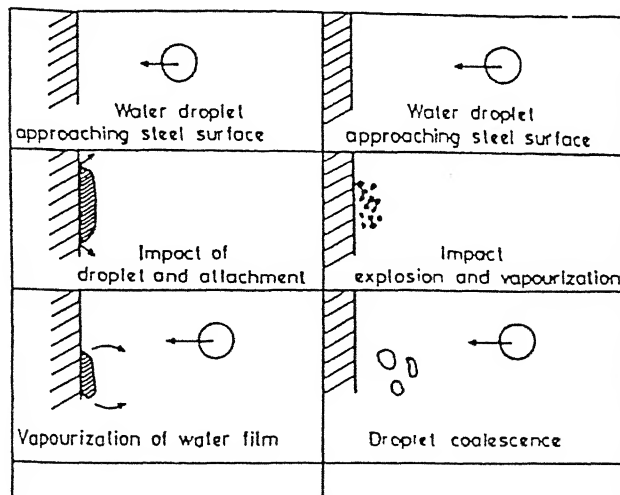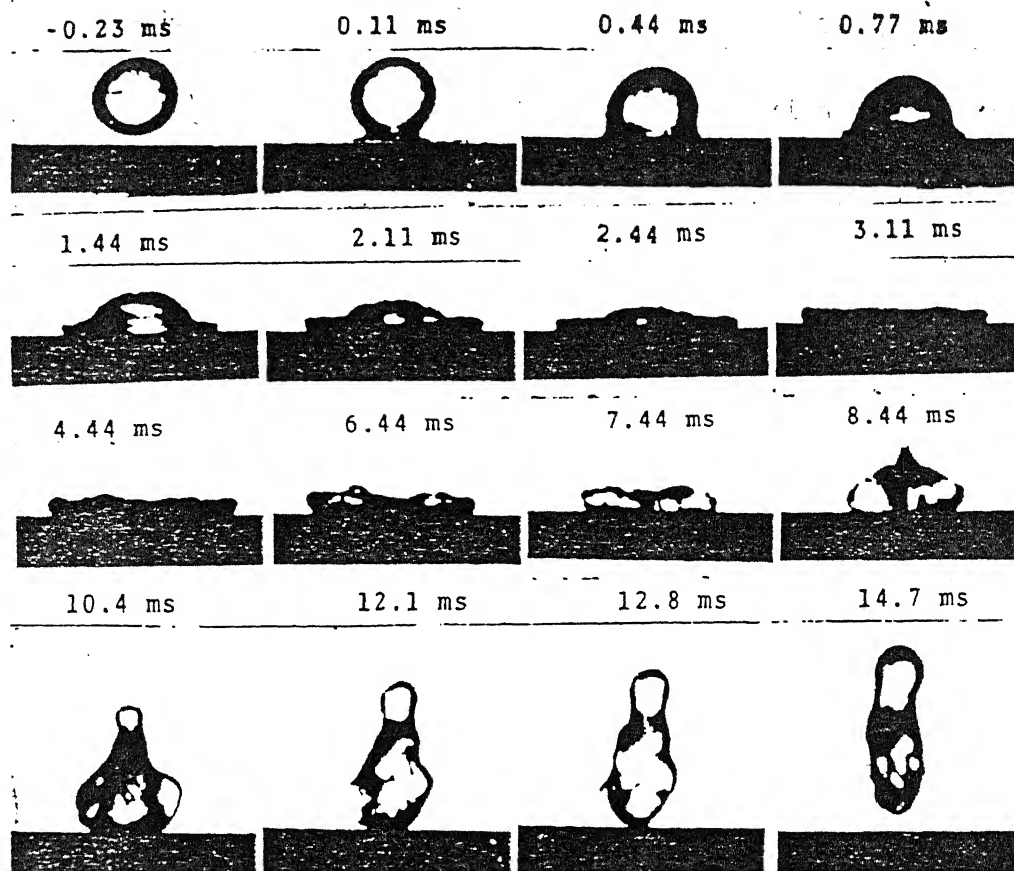
400°C, $2r_0 = 0.29$ cm,
6 cm/sec, $We = 30$
after the moment of
contact is indicated.

Fig. 2.13 Course of the impact of a water droplet.

behaviour exhibited in the Fig. (2.14) and it shows the heat flux density as a function of the boiling temperature. The ranges of 1) free convection 2) nucleate boiling, 3) partial film boiling and 4) stable film boiling should be distinguished [15]. In the spray water cooling, these will run from higher to lower temperature. The cooling of the steel begins in the range of stable film boiling, where by a stable vapour film forms between the metal and the liquid spray water. If the Leidenfrost temperature is reached, this vapour film partially collapses. Further cooling takes place in the range of partial film boiling, whereby water droplets partly moisten the surface of the metal This is connected with the considerable rise in the heat-flux density.

2.5.2 Leidenfrost Temperature [16]

When a water droplet contacts to a hot surface, with the temperature well above $100^{\circ}C$, boiling will occur. For single droplet resting on a horizontal surface the Leidenfrost phenomena is well known. Above a certain temperature, the temperature T_D, a vapour cushion is formed between drop and surface, reducing heat transfer appreciably. above this temperature water surface does not wet the surface. As soon as wetting starts just below T_D a sudden strong steam generation occur. However, transition at this temperature is not so sharp and well defined as for single droplet. T_D can be raised to much higher values than for a single droplet. Density and velocity of impinging water droplets increase the Leidenfrost temperature.

2.6 HEAT TRANSFER STUDIES

Spray heat transfer coefficients are affected by a large number

Fig. 2.14 Mechanism of heat transfer in pool boiling.
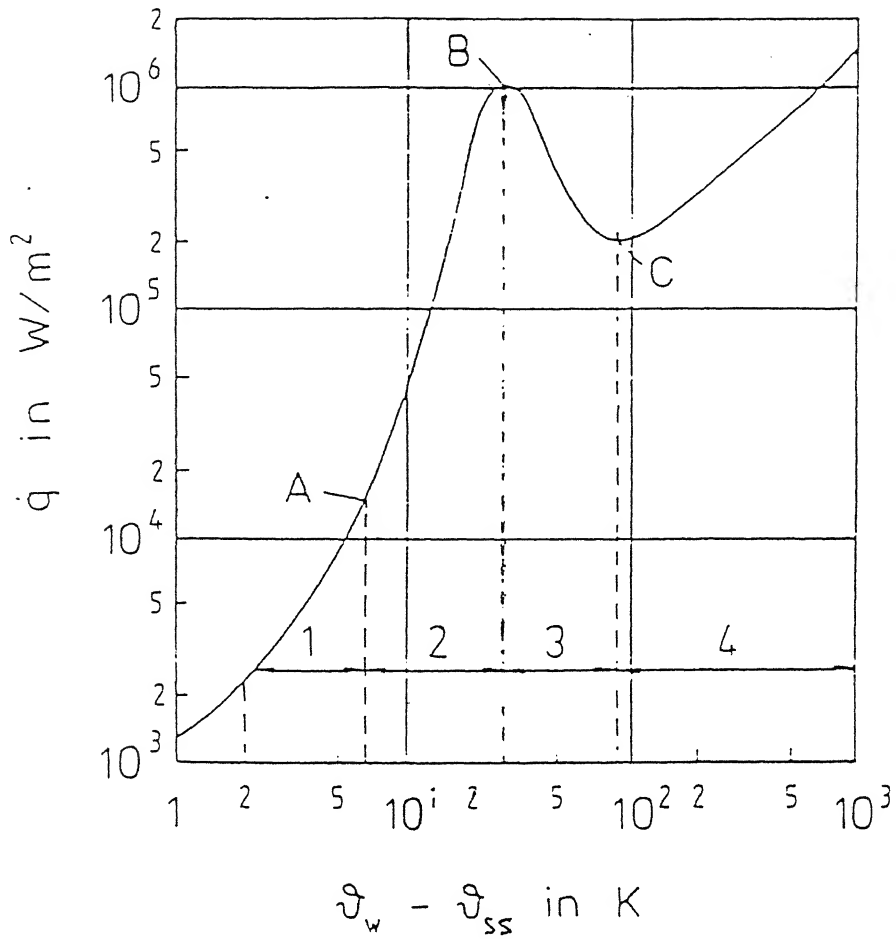
1. free convection
2. nucleate boiling.
3. partial film boiling
4. stable film boiling

of variables such as nozzle type, nozzle to strands distance, water pressure, water temperature, surface temperature of steel etc. To simplify matters, these variables can be divided into two categories depending on whether or not they influence the spray-water, which, as will be seen, is the most important variable. Thus, the effect of variables such as nozzle type water pressure and nozzle-to strand distance on spray heat transfer can be seen primarily in terms of their effects on flux, where as variables like water temperature and steel temperature affect heat transfer directly [17].

Most of the authors have done work in heat transfer studies during cooling. Variables which affect the transfer of spray cooling are given in the following:

1) Surface temperature

2) Initial temperature

3) Water flux

4) Sample size

5) Specimen surface properties

6) Thermophysical properties

2.6.1 Effect of Surface Temperature

Under normal continuous casting conditions, in which the surface temperatures range between $1200^{\circ}C$ and $700^{\circ}C$, surface temperature has only a small effects on the heat transfer coefficient [18]. According to Mizikar [10] increase in surface temperature causes heat transfer coefficient to decrease slightly. The small effect has also been reported by Muller and Jescher [19]. Mitsutsuka et al have found that the heat transfer coefficient is proportional to $T_s^{-1.2}$. The relative lack of dependence of h on T_s is characteristics of the film boiling region of the classical

boiling curve. At lower surface temperature, below $550^{\circ}C$, the h value increases sharply as nucleate boiling begins to take effect. h_w is little influenced by T_s when $T_s \geq 600^{\circ}C$ [4], since as for the droplets ejected onto the upper surface of the specimen are heated, immediately after impinging against the surface in the Leidenfrost state and then fall from the specimen. The heat transfer from the specimen to the water droplets includes, sensible heat for heating up to boiling point and latent heat for evaporation. The amount of heat transferred during the period from the time, the water droplets impinge on the hot specimen till the time they reach the Leidenfrost stage in large. However once the water droplets have reached the stable Leidenfrost state, the amount of the heat transferred to them is small, though the evaporation rate is slightly increases in proportion to T_s. For these reasons, h would be little influenced by T_s insofar, T_s is sufficiently high [4,19].

2.6.2 Effect of Water Flux

The critical (Leidenfrost) temperature below which the heat transfer coefficient rises rapidly, has been shown to increase with water flux [20].

All studies agree that, in the temperature range of interest, the spray water flux, $\dot{w}$ has the largest effect on the heat transfer coefficient. The experimental findings of the different studies are shown that the relationship (except [21]) is reported to be nonlinear

$$h \propto (\dot{w})^n$$

Most workers agree that the value of n lies between 0.5 to 1.0 Nilles et al, for eg., have found that n decreases from 1 to 0.5, when the spray flux increases from 2 to 20 $Lm^{-2}s^{-1}$. The fractional value of n indicates, of course, that an increase in water flux has less than a

proportional effect on the heat transfer coefficient. But according to Narasaki et al. [15], $h \propto \dot{w}^{1.2}$

According to Mitsutsuka and Fukuda [3] $h_{mist} > h_{water\ spray}$ for same amount of water flux. $h \propto \dot{w}^{0.8}$ for lower velocity of air. For higher V_a values, conducted by Kunioka et al. [20] and the test with high T_s values conducted by Yanagi et al. [9]

$$h \propto (\dot{w}\ V_a)^n$$

$$n = 0.36 \text{ (from [20])}$$

$$n = 0.75 \text{ (from [3])}$$

The relationship between the rate of heat extraction by water sprays and the spray variables, which influences defect formation, has been established in a number of experimental studies [10, 21-25] and in Table 2.1, these are given in detail.

Since the heat transfer coefficient is the most useful parameter with which to characterize the effectiveness of heat extraction for the purpose of spray design [10]. According Jescher et al. [19] water flux density i,e. the water quantity, which is supplied to the surface per unit time and per unit surface, is besides the surface temperature very important for the heat transfer. It has been proved that all parameters, like nozzle pressure, volume flow as well as the nozzle distance from the surface of the test sample, can be combined in this quantity. In the range of stable film boiling the heat transfer coefficient h increase with rising water flux density. According to Mizikar [10], h was found to increase linearly with increase in water flux. A four-fold variation in h was obtained by changing only the water flux.

2.6.3 Effect of Sample Size

The advantage of the small size of the sample lies in the

able 2.1   : Correlations between h and w for water spray and mist
              cooling available in literature.

dy	Method used to obtain h	Correlation	Comments
:sutsuka [18]	Mist cooling horizontally placed steel plate. w: 5 to 68 L/m²min heated in electrical furnace to 900°c Specimen (mm) : 400x800x28	$h(KCal/m^2 h °C)$ $\alpha (wv_a) 0.8$ in range to T_s 600° to 150° c V_a=7 to 10 m/sec	Radiation par included
nagl et al.[18]	Mist Cooling w: 15 to 50 L/m²min Steel Specimen (mm): 5x30x0.2 t	$h(KCal/m^2 h °C)$ $\alpha (wv_a) 0.8$ in range of T_s 900° to 700° c V_a=5 to 9 m/sec	
nioka et al.[18]	Mist Cooling w:300 to 960 L/m²min Specimen in unknown	$h(KCal/m^2 h °C)$ $\alpha (wv_a) 0.36$ in range of T_s 600° to 200° c V_a=300 to 200 msec	
cler & Jeschar ?]	Cylindrical sample of 30 mm dia. heated upto 850°C unsteady state. T_w=20°C $\dot{m}_s$ 100 to 1000 Kg/m².min.	$h (w.m^2/°K)$ = 1.82 ms (Kg/m².min) + 198 in range of stable film cooling.	Radiation is included. Correlation is valid bot for mist and water spray. It is independent of metal in stable film boiling reg
Ima Combe [20]	Air-water spray cooling steel plates cooled under transient conditions and operating continuous casting machine. T_w=25° and strand temp. is 1000°C	$h (kw/m^2)$ = 0.35 w $(L/m^2.s)+0.13$	Radiation component subtracted.
izi et al. [20]	Mist cooling small cylindrical steel sample heated to 1050°C. w:20 to 2000	$h (KCal/m^2 .h °C)$ $=(a.A/w+b)w^{1.2}+C$ A/w: air/water T_s in the range of 1000°C to

assessment of nozzle properties in respect of heat transfer [15]. Measurement of heat transfer takes place in the range of stable film boiling, i.e, at surface temperature above $600^{\circ}C$. For cooling the customary steel strand dimensions, this is the interesting surface temperature range. There further advantage that, in accordance with the heat transfer coefficient during stable film boiling is independent of the surface temperature. This means that the heat transfer coefficient measured in this stage can be used directly for the calculation of the heat transfer in the secondary cooling zone of continuous casting machines.

2.6.4 Effect of Specimen Surface Properties [4]

1. T_s corresponding to maximum value h_{max} of h is shifted towards the higher temperature side as the amount of scale deposit increases.

2. The value of α_{max} decreases as the amount of scale increases.

3. In the mist cooling of a hot steel plate with scale deposit, the value h increases in proportion to the amount of scale deposit in the region where $\dot{w}$ is small and its surface temperature is over about $200^{\circ}C$.

2.6.5 Thermophysical Properties

Jescher et al. [19] had used four different materials with different properties to examine the influence, which the properties (heat conductivity k, density ρ, and specific heat C_p), important for the heat transport, have on the heat transfer coefficient. They reported that Copper, Nickel, Aluminium and Brass 37 have no effect on the heat transfer in the range of stable film boiling. But Leidenfrost temperature depends on properties of the material. According to them, heat flux density $\dot{q}$ is

proportional to the intrusions coefficient; so that following in valid

$$\dot{q} \sim \sqrt{k \, \rho \, C}$$

The curve of the Leidenfrost temperature moves to smaller value with increasing intrusion coefficients and constant water flux density.

2.7 OBJECTIVE OF THE PRESENT WORK

An experimental study on the characterization of mist and water spraynozzle, is carried out in the present work, along with the study on behaviour and nature of spray under various conditions.

The effects of water pressure, spray distance and the nozzle design on the spray are observed and discussed here.

Heat extraction capability of nozzle and influence of other variables like initial temperature, thermophysical properties, water flux etc. on the the same are studied and elaborated later on. The effect of heat extraction capability observed by means of two routes - one is study of heat transfer, the other one is study of quenching of hot metal surfaces. The relevant observations related to quenching like changes in microstructure and hardness are also made subsequently.

CHAPTER 3

EXPERIMENTS

This chapter deals with the experimental set-up and procedure for characterization of nozzles and heat transfer studies. These are described in the following sections.

SET-UP

The set-up for the characterization of nozzles is shown in Fig. . Fig. 3.2 gives the sectional view of mist and water spray nozzle. . 3.3 shows the schematic diagram of the experimental set-up for the dies related to heat transfer. For all the studies, tap water ($\sim 27^{\circ}$C) used and air is taken from the compressor.

.1 Design of Mist Nozzle

Two different types of nozzles are used: mist and water spray. design of both the nozzles is shown in Fig. (3.2). Fig. (3.2a) shows design of different parts of mist nozzle. These are: air and water ply, nozzle head and a cap. Air and water are supplied through the pipe the nozzle head consists of flow passage for water and air. A hole of m diameter is in the center of the nozzle and water flows through this e where as six angular holes of diameter 2 mm are arranged cumferentially over the water nozzle. Air flows tangentially with pect to water stream and just outside the nozzle the mixing takes place h the water. The pressure gauges are mounted to measure the inlet ssure of water and air. Volumetric measuring flask is used to measure water flow rate.
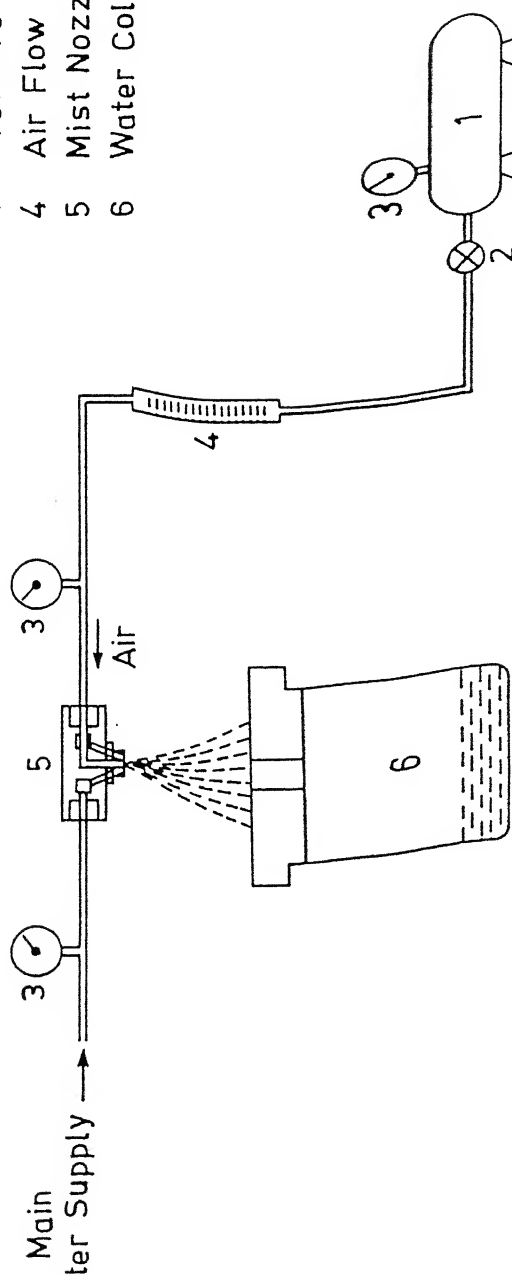
Fig. 3.1 Set-up for the characterization of nozzle.
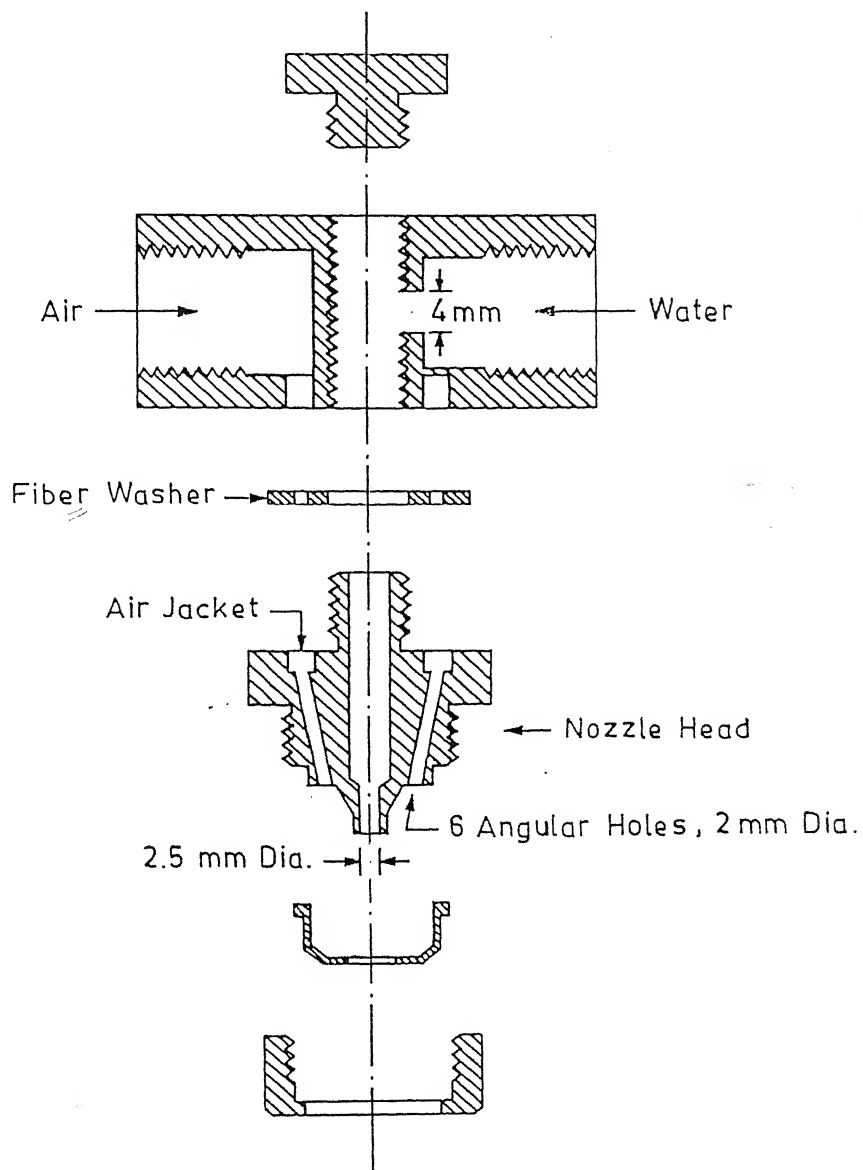
a) Mist Nozzle Assembly
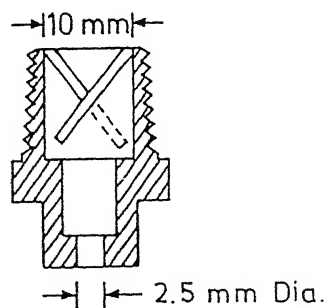
b) Full Cone Water Spray Nozzle

Fig. 3.2 Sectional view of the mist and water spray nozzle.
(a) Design of different parts of mist nozzle.

3.1.2 Design of Water Spray Nozzle

The design of water nozzle is schematically shown in Fig(3.2b). From the figure, it can be seen that the water inlet pipe has diameter of 10 mm and the outlet diameter of the nozzle is 2.5 mm. The water nozzle is designed in such a way to produce a full cone of water spray.

3.1.3 Heat transfer studies

The set-up for the studies regarding heat transfer is shown schematically in Fig(3.3). Two different shapes of steel samples, cylindrical and rectangular (dimensions are given in Fig(3.3))are used. The mist region is chosen for the heat transfer studies. Some of the experiments are also carried out for the water spray. Tube furnace is used to heat the sample to the desired temperature. Samples are homogenized for one hour. After the attainment of the particular temperature, sample is taken out of the furnace and cooled vertically under the mist or spray. In order to measure the temperature at two positions, thermocouples are embedded in the specimen at the positions $r=0$ and $z=2.5$ and 41.5 mm as shown in Fig(3.3). The K-type (Chromel-Aluminel) thermocouples are used to measure the temperature. The cold junction of the thermocouples are connected to the interface, i.e. **PCL 212 Thermocouple Input Card**, with the microcomputer.

3.1.3.1 Thermocouple input card

The PCL 212 thermocouple input card with dual integration type analog to digital converter gives excellent channel to channel isolation through the Reed Relay Multiplexer. Built in cold junction compensation makes it easy to interface with the thermocouple directly with the ice bath. Analog to digital conversion can be initiated by software triggering or internal programmable timer triggering. This card also gives provisions

1   Nozzle
2   Mist
3   Test Sample
4   Thermocouple
5   PCL 212 Interface Card
6   Micro Computer
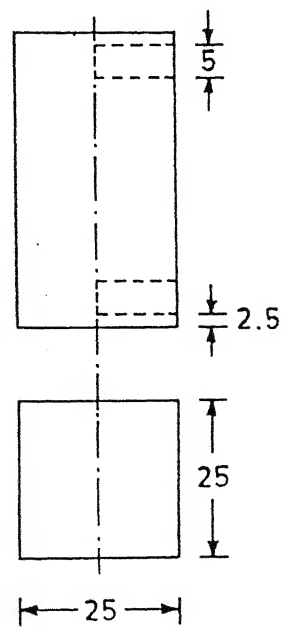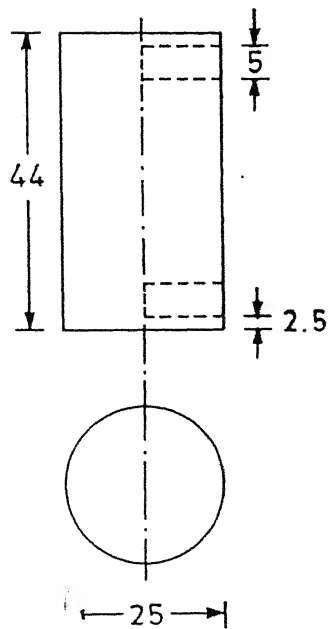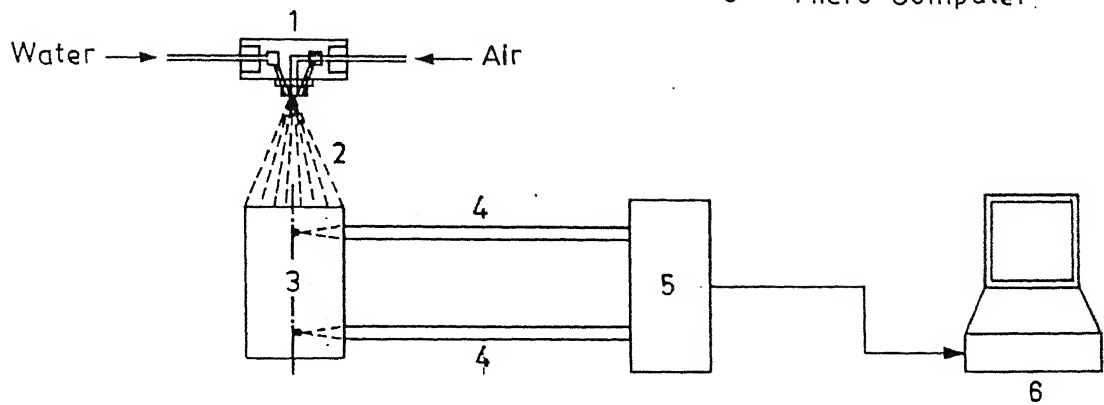
Dimensions in mm

for detecting the end of conversion by polling or through interrupt. A variable gain amplifier is provided to facilitate interfacing with different type of thermocouples. This card is calibrated for the present environment.

3.2 EXPERIMENTAL PROCEDURE

The experimental procedure and the experimental variables for the characterization of nozzles, heat transfer and effect of quenching of hot metallic surface are discussed here respectively.

3.2.1 Nozzle Characteristics

Full cone mist nozzle and water spray nozzle are considered for the present study. To observe the behaviour of the spray and the distribution of flux in spray, the following experimental variables are chosen

1) Air flow rate

2) Water flow rate

3) Spray distance

The above three variables will effect the water flow characteristics, air flow characteristics, structure of two phase flow and the flux distribution in spray correspondingly.

i) Water Flow Characteristics

The effect of water flow rate on the water pressure is studied for both the nozzles. The water flow rate is measured with a volumetric measuring flask and the pressure is noted from the pressure gauge. The quantity of water is collected for a particular length of time (10 sec. to 60 sec.) and converted into the unit of $Lmin^{-1}$. Pressure is noted in unit of $Kg\ cm^{-2}$ and it is converted into KPa G. For the increase in the water

flow rate, water pressure is noted. All the measurement are repeated for three times and the mean values are taken. The amount of water is varied from 0.135 to 2.560 L min^{-1} for mist nozzle and for water nozzle the range is 1.280 to 3.880 L min^{-1}.

ii) Air Flow Characteristics

Rotameter is used for the measurement of air flow rate. Rotometer is calibrated for NTP and in the unit of NLmin^{-1}. Pressure gauge is mounted to note the pressure. For the single phase flow of air, the effect of air flow rate is varied from 20 NLmin^{-1} to 160 NLmin^{-1}. Then the water is allowed to pass through the nozzle. In this two phase region, again the effect of air flow rate on the air pressure is studied. The amount of water is varied from 20 NLmin^{-1} to 160 NLmin^{-1}. These measurements are repeated.

iii) Mist Characterization

The formation of mist is studied by varying the water and air flow rates and by the visual observations. At constant flow rate of water, increase in air flow rate enhances the disintegration of water stream. The two phase jet can be called as 'mist', only when very fine water droplets are observed to be distributed evenly in the two phase jet. Increase in water flow rate is found to increase the air flow rate for the above observations. Water flow rate is varied from 0.2 to 2.8 Lmin^{-1} and air flow is varied from 20 to 160 NLmin^{-1}. At some particular air flow rate, minimum and maximum amount of water needed for the formation of mist is measured. For all the air flow rates, the measurements are carried out and the values are noted.

3.2.2 Heat transfer studies

The specimen with thermocouples are heated in the tube furnace to the desired temperature and homogenized for the uniform temperature. The

specimen is taken out of the furnace and held vertically below the mist or water spray. Water flux in the mist for these experiments is determined by measuring the volume of water collected in a container whose diameter of the mouth is same as the sample diameter(25 mm). The flux is calculated by the amount of water collected in the container per unit area per unit time. Water flux can be varied by changing the air,water flow rates and the spray distance. The cold junction of the thermocouples are connected to the PCL 212 Thermocouple input card with the microcomputer. The performance of the card is given in section 3.1.3.1. During cooling, temperature of the sample with respect to time can be directly recorded and stored in the microcomputer. The software which is used for recording the variation of temperature with time during cooling is given in Appendix A. The temperature in mV is then changed into $^{\circ}$c by another executable program. These temperature-time values are used for the calculation of heat transfer coefficient. In Appendix B, the basic theory behind the calculation of heat transfer coefficient, the need for the numerical solution by FEM and the program which is used to calculate the heat transfer coefficients,are given. Initial temperature of the specimen just before cooling and temperature of water inlet are noted.

3.2.2.1 Data acquisition system

On line measurements for the recording of temperatures during cooling of hot surfaces can be performed through a data acquisition system. The interfacing of the thermocouples are done with the PCL 212 Thermocouple input card with the microcomputer. The performance of the card is given in section 3.1.3.1. Since two thermocouples are used in the present study, two out of eight channels are selected for the measurement of emf produced by the thermocouples. One channel is for the thermocouple at the position r=0, z=2.5 mm and the other channel for the thermocouple at the position

r=0, z=41.5mm. The input card is calibrated for the present study. The readings which are obtained via this interfacing card are then changed in to temperature in degree celsius.

3.2.2.1 Experimental variables

For the nozzle characterization, water and air flow rates are the experimental variables.

Water flow rate: 0.1 to 2.56 Lmin^{-1}for mist nozzle

1.3 to 3.90 Lmin^{-1}for water spray nozzle

Air flow rate : 20 to 160 NLmin^{-1} for mist nozzle

For the heat transfer measurements the experimental variables selected are,

1. Initial temperature of the specimen

2. Water flux (by varying Q_w,Q_a and x_o)

3. Radiation

4. Reheating

5. Thermophysical properties

6.Type of cooling

1. Initial temperature:

The water and air flow rates are kept at 1.120 Lmin^{-1}and 140 NLmin^{-1} respectively. The sample is cooled at a predetermined spray distance. The initial temperature of the specimen is varied from 600°c to 900°c

2. Water flux:

The initial temperature of the sample is kept at 800-827°c. The water flow rate is varied from 1.120 to 2.280 Lmin^{-1} air flow rate is varied from 130 to 150 NLmin^{-1} and spray distance is varied from 26 to 222 mm.The same range of water flow rate is chosen for the water spray.

3. Radiation:

The water,air flow rates,spray distance and the initial temperature are kept constant. The sample is shielded by the insulating material (Alumina powder mixed with orthophosphoric acid), except on the surface which is facing the mist.

4. Reheating:

The other experimental variables are kept constant. The sample which is cooled once under the mist is reheated again and cooled in the mist. After second cooling the sample is reheated for the third time and then subsequently cooled.

5. Thermophysical properties:

Mild steels(0.2% C), medium carbon steels(0.7% C), high carbon steels (1.5% C),and copper and brass(70% Cu and 30% Zn) samples of the same dimensions are taken. For the steel and copper samples the initial temperature is fixed at 800-827°c and for the brass samples the initial temperature is 600°c.

6. Type of cooling:

The initial temperature and the air,water flow rates are kept constant. Three type of cooling are employed :air,water spray and mist. For both water spray and mist cooling the water flow rate is fixed to 1.120 Lmin^{-1}. The air flow rate for mist and air cooling is 140 NLmin^{-1}. The spray distance and initial temperature of the samples are same for all the types of cooling.

3.2.3 Studies on quenching

Plain carbon steels are heated in the tube furnace to 802°c and soaked for one hour. The samples are cooled by mist, water spray, and quenched in water. Hardness measurements are performed for the samples in Rockwell Hardness Tester. To observe the effect of cooling, the hardness

values are taken at various depths from the cooling end, i.e, at positions r = O and z = 1 mm to 44 mm..

To observe the structural changes during cooling, the samples are ground,polished, etched and photographs are taken under the Optical Microscope.

CHAPTER 4

RESULTS AND DISCUSSION

In this chapter, experimental results regarding the characterisation of nozzles, heat transfer studies and quenching, are presented and discussed respectively in the subsequent sections.

4.1 BEHAVIOUR OF NOZZLES

4.1.1 Water Flow Characteristics

The nozzle behaviour is studied by pressure - flow rate relationships. In Fig.(4.1), the variation of inlet water pressure P_w with the water flow rate Q_w is given for water and mist spray nozzle. The data are given in Table 4.1. From the figure, it can be observed that increase in water flow rate increases the water pressure for both types of nozzles. For example, when Q_w increases from 1.0 to 3.0 $Lmin^{-1}$, the pressure drop increases from 20.0 to 90.0 kPa G for mist nozzle. Whereas for the water nozzle, this pressure drop increases from 5.0 to 30.0 kPa G.

This behaviour is due to the design of inlet and outlet cross sectional area of the nozzle. Both the nozzles have identical outlet diameter (2.5 mm). In case of mist nozzle diameter of inlet water supply is 4.0 mm, but for the spray nozzle, it is around 10.0 mm. For a same flow rate and same outlet diameter, a smaller inlet obviously results in larger pressure drop as compared to the larger one.

The above results point out the importance of the selection of the appropriate dimension of the inlet and outlet of the nozzles. If larger pressure drop is required with small amount of water (as in the case of mist nozzle) then the difference between the inlet and outlet diameter

Table 4.1 Pressure-Volume flow rate data for water for water spray and mist nozzle.

Mist nozzle		Water nozzle	
Water flow rate Q_w (l/min)	Water press. P_w (KPa)	Water flow rate Q_w (l/min)	Water pressure P_w (KPa)
0.135	2.37	1.28	5.880
0.345	2.94	1.62	7.840
0.520	5.83	2.30	12.544
0.680	9.16	2.64	17.836
0.800	9.80	2.72	19.796
0.880	15.43	2.84	25.088
1.030	23.82	3.16	27.244
1.240	31.55	3.32	31.850
1.380	38.48	3.48	33.320
1.490	44.88	3.52	35.280
1.760	49.00	3.68	37.044
1.940	55.80	3.70	39.200
2.080	63.70	3.74	42.140
2.280	75.52	3.88	44.100
2.320	88.69	—	—
2.560	93.10	—	—
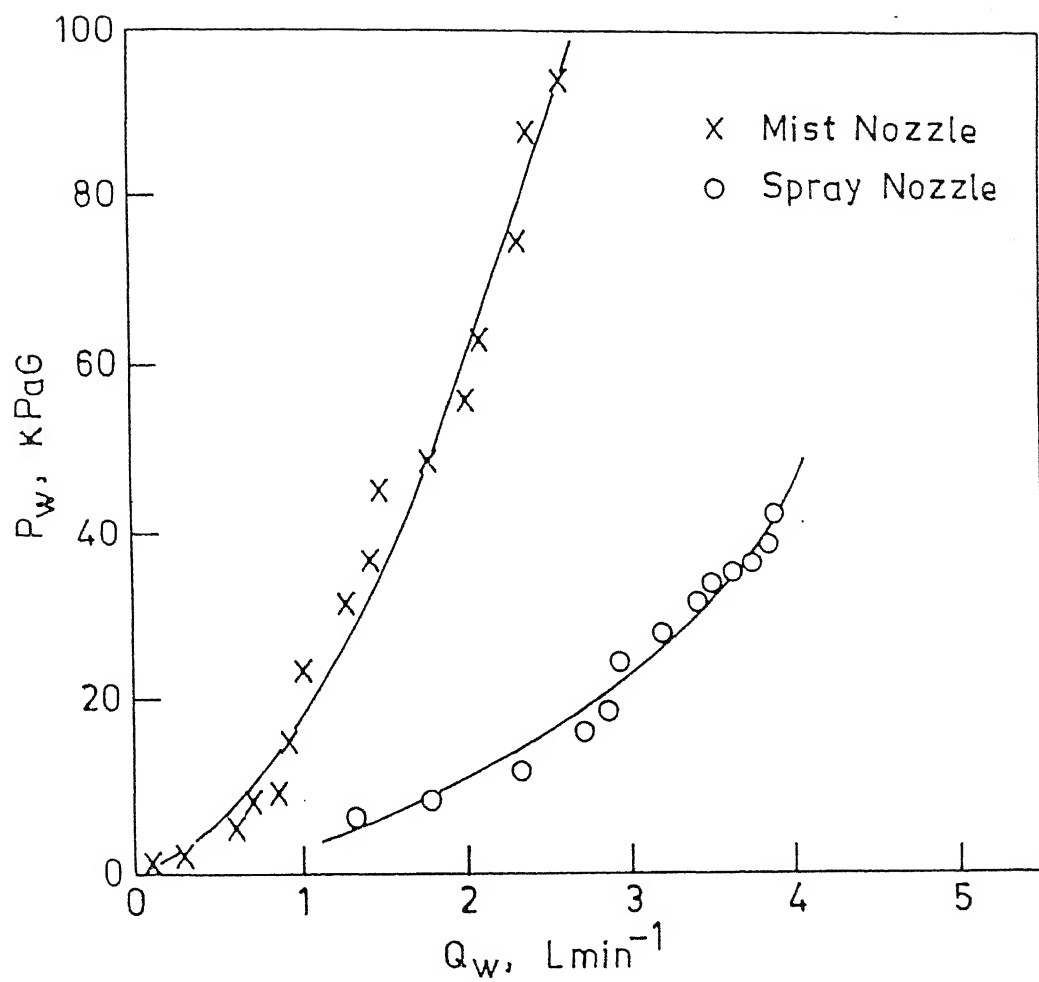
Fig. 4.1 Water flow characteristics.

4.1.2 AIR FLOW CHARACTERISTICS

The air flow rate characteristics is investigated only for the mist nozzle. In Fig.(4.2), the variation of air inlet pressure P_a is noted air flow rate Q_a; for three different flow rate; 0.88 $Lmin^{-1}$, 1.15 $Lmin^{-1}$ and 1.32 $Lmin^{-1}$. The plot also contains the pressure - flow rate relationship for air only. Table 4.2 gives the data for air flow characteristics. It can be seen in the figure that increase in Q_w increases the P_a.

In the figure, the influence of Q_w on P - Q characteristics is shown by the bar. The height of the bar represents the range of pressure variation for a given flow rate. Within 20.0 to 90.0 $Lmin^{-1}$ of air flow rate, the height of the bar represents the variation in P_a of the order of 5 kPa G, when water flow rate is increased from 0.88 to 1.32 $Lmin^{-1}$, whereas in the range of 90.0 to 160.0 $NLmin^{-1}$, the height of the bar represents the variation in P_a of the order of 30 kPa G for the same water flow rates.

In the mist nozzle design, the mixing of air and water controls the pressure drop of the mixture. When water and air are mixed in the nozzle, then the Q_w influences the pressure drop for the flow of air [27]. However, when water and air flow through different holes and mixes down stream the nozzle, as in the case of present mist nozzle design, then the water flow rate should not influence the pressure drop for air flow. But the relatively small effect of Q_w on P_a is considered to be due to the resistance offered to the flow of air by the water flow.

4.1.3 Two Phase Flow Structure

When water and air flow simultaneously through a nozzle, two

Table 4.2 Effect of water flow rate on air pressure when water and air flow simultaneusly through the mist nozzle.

| Air flow rate Q_a (Nl/min)	Air pressure without water, P_a (KPa)	Air pressure with water, P_{aw} (KPa)		
		P_{aw1} (Q_w = 0.88 L/min)	P_{aw2} (Q_w = 1.15 L/min)	P_{aw3} (Q_w = 1.32 L/min)
0	0	0	0	0
20	9.80	9.80	9.80	9.80
30	14.70	15.20	15.20	15.20
40	19.60	20.58	22.54	20.58
50	28.42	28.44	28.42	27.44
60	34.30	42.14	42.20	42.20
70	44.10	44.10	44.10	44.10
80	56.84	56.90	56.84	56.84
90	76.44	80.21	80.21	80.21
100	88.20	96.04	117.60	117.60
110	129.36	132.30	132.30	134.26
120	174.44	181.30	186.20	188.16
130	210.70	225.40	235.20	237.16
140	274.40	274.40	284.20	284.20
150	321.44	333.20	343.00	343.00
160	382.20	392.00	401.80	401.80
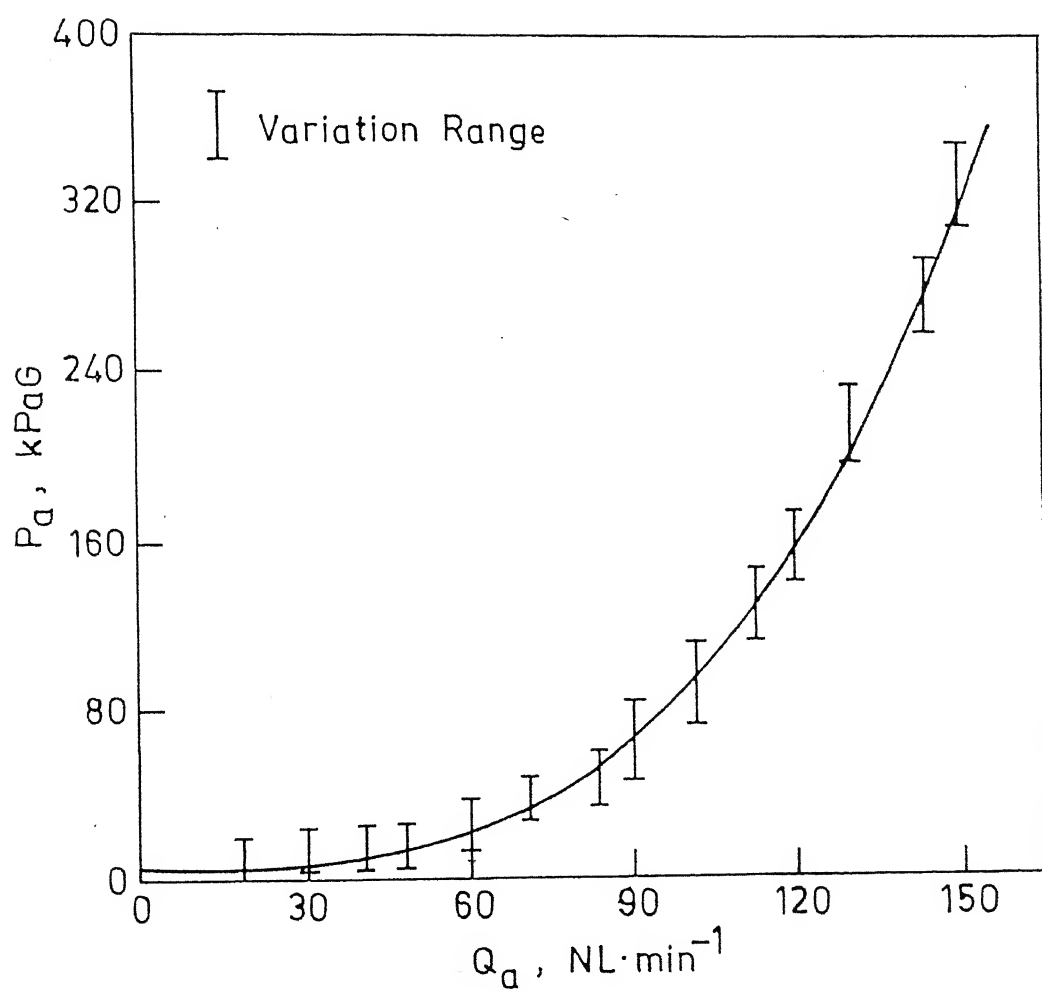
Fig. 4.2   Air flow characteristics.

phase jet is formed in the down stream of nozzle. Visual observations have shown that the structure of the two phase flow depends on the air - water range. Fig.4.3 shows the variation of Q_a with Q_w and the classification in the various types of two phase flow and these are denoted by A,B,C and D. It should be mentioned here that the boundary of each type of two phase flow is determined by the visual observations. Experimental data are reported in Table 4.3.

Partial water jet :

In the Fig.4.3, 'A' denotes the region of partial water jet. In this region, the air flow rate is small and it flows tangentially to the water stream, which results in the production of very few water droplets from that periphery of water stream. Occurrence of disintegration of main water streams into water droplets is not observed. The two phase mixture contains very few droplets of water, air and water. In this region any combination of water and air flow rate is found to be insufficient to disintegrate the water stream fully.

Coarse mist :

Coarse mist region is denoted by 'B' in Fig.4.3. For the increase in Q_a, the water stream begins to be atomised into water droplets. The size of the water droplets has been observed to be large. At particular air flow rate, the mixture consists of coarse water droplets moving with air. The required amount of air depends on the water flow rate or vice versa. Increase in water flow rate increases the need for larger air flow rate.

Mist :

This region is denoted by 'C' and the hatching in this region shows the lower and upper limits of water flow rate which can be converted into mist by a given air flow rate. Mist can be defined as the two phase jet which consists of very fine droplets distributed in the air jet. The

Table 4.3 Experimental data on air and water corresponding to mist jet formation; $(Q_w)_{min}$ and $(Q_w)_{max}$ correspond to lower and upper limits of water flow rate.

| Q_a (NLmin^{-1})	$(Q_w)_{min}$ (Lmin^{-1})	$(Q_w)_{max}$ (Lmin^{-1})	Turndown Range
80	0.185	0.414	2.237
100	0.320	0.625	1.953
110	0.380	0.980	2.578
120	0.430	1.250	2.906
130	0.480	1.730	3.604
140	0.640	2.300	3.593
150	0.750	2.420	3.226
160	0.920	2.560	2.782
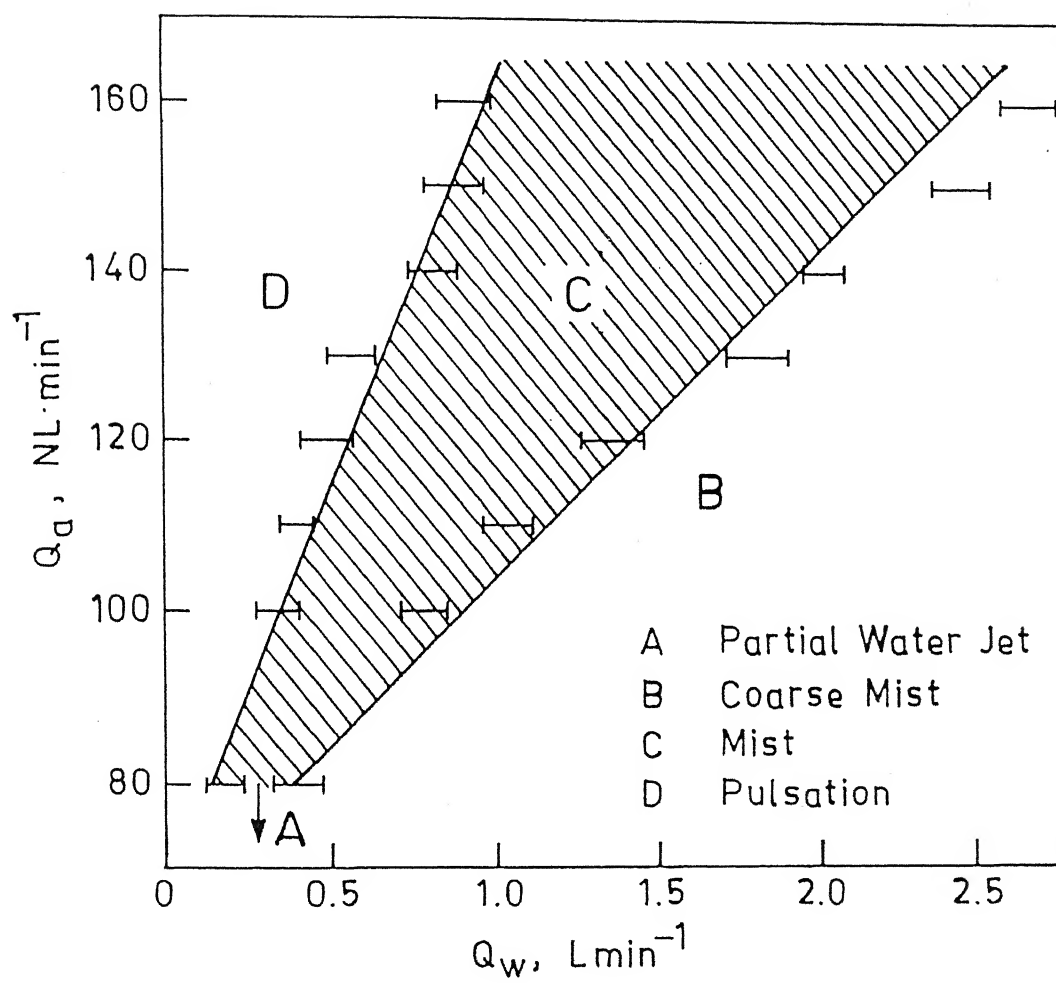
Fig. 4.3 Two phase flow structure diagram.

maximum and minimum water region increases with the increase in the air flow rate. For example, 100 NLmin^{-1} of air flow rate requires minimum of 0.4 Lmin^{-1} of water to form the mist and the same amount of air can convert 1.0 Lmin^{-1} into mist. But the minimum and maximum limits of water rate at 150 Lmin^{-1} are 0.75 and 2.42 Lmin^{-1} . The ratio between the minimum and maximum water that can be converted to mist is 1.95 at 100 NLmin^{-1} and increases to 3.22 at 150 Lmin^{-1}.

Pulsation :

Region 'D' in the figure represents the pulsation which is formed in the two phase flow jet. For the given water flow rate, if the air flow rate is increased above a certain value, pulsation in the two phase flow is noted. It is also observed that the mist is no longer stable. Both decrease in water flow rate and increase in air flow rate result into pulsation.

Optimum value of water flow rate needed to form the mist at particular air flow rate is shown by the hatched region in Fig.4.3. For the optimisation of air and water flow rates the selection of nozzle diameters and the design of nozzle are some of the important factor.

4.1.4 Water Flux

In the experiments, amount of water in the mist is measured as a function of air and water pressure and the down stream distance. The amount of water collected by allowing the mist to pass through a hole of 25 mm diameter. This hole diameter is corresponding to the diameter of cylindrical specimen.

The calculated values of flux and other relevant variables are given in Table 4.4. The experimental results are analysed by the following functions.

Table 4.4 (a) Effect of water and air flow rate and spray distance on water flux for mist nozzle.

	Q_a (NL/min)	Q_w (L/min)	x_o (cm)	$\dot{q}_w$ (Lm^{-2}s^{-1})
Variation in Q_w	140	1.120	8.2	32.59
	140	1.820	8.2	46.85
	140	2.280	8.2	63.15
Variation in Q_a	130	1.120	8.2	36.67
	140	1.120	8.2	32.59
	150	1.120	8.2	30.56
Variation in x_o	130	1.240	8.2	38.20
	130	1.240	14.2	28.56
	130	1.240	22.2	20.32
	140	1.980	2.6	59.08
	140	1.980	4.9	55.00
	140	1.980	8.2	48.89
	140	1.980	14.2	40.74

Table 4.4 (b) Effect of flow rate and spray distance on water flux for water spray nozzle.

Q_w (L/min)	x_o (cm)	$\dot{q}_w$ (Lm^{-2}s^{-1})
2.28	8.2	28.52
1.82	8.2	20.37
1.12	8.2	10.19
0.90	8.2	8.49
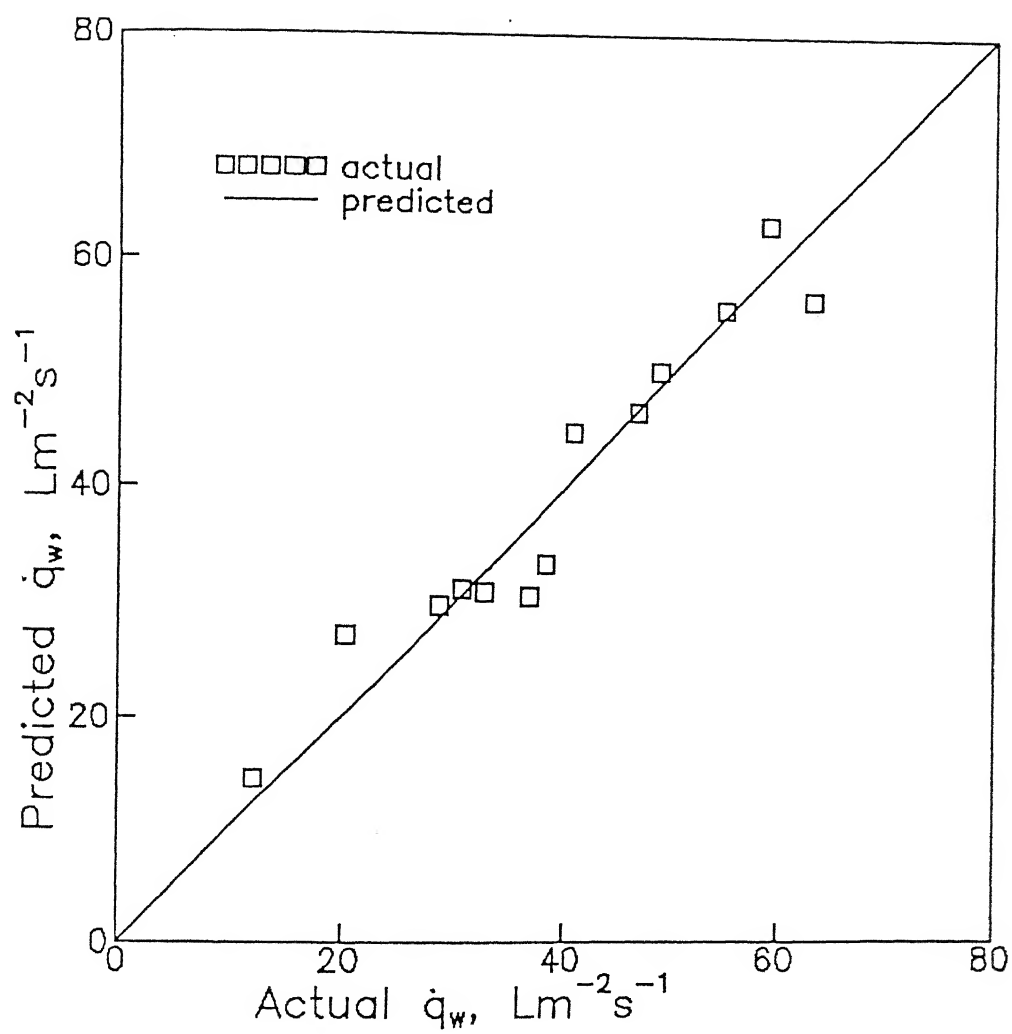
ig. 4.4 Variation of water flux ($\dot{q}_w$) with water and air flow rates and spray distance, plotted by multiple regression analysis.

$$\dot{q}_w = A \ (Q_a)^m \ (Q_w)^n \ (x_o)^p \tag{4.1}$$

The values of preexponents and the exponents are determined by the multiple regressions analysis. With those values, the following equation results.

$$\dot{q}_w = 130.2192 \ (Q_a)^{-0.1419} \ (Q_w)^{0.8995} \ (x_o)^{-0.2} \tag{4.2}$$

The Eqn.(4.2) is plotted in Fig.4.4 and this equation describes satisfactorily the experimental data points. From the Eqn.(4.2) it is observed that the increase in water flow rate increases the flux and decrease in air flow rate and the spray distance increase the flux.

4.2 HEAT TRANSFER

Results of the heat transfer measurements for steel, copper and brass are given and discussed in this section. During the cooling, the temperature of the sample at two different locations are measured and recorded continuously on the microcomputer. Cooling curves for all the experimental variables are given in the following sections. In the cooling curves, solid line represents the variation of temperature with time at positions r = 0.0 and z = 2.5 mm and the dashed line that of the position r = 0.0 and z = 41.5 mm. It can be seen in the figure that the cooling rate is different at various position; surface which is facing the mist cooled faster than that of the farther one.

Most of the heat transfer experiments are carried out for mist only. For the comparison of water spray with mist, some experiments are conducted with water spray also.

From the temperature versus time data heat transfer coefficient is calculated. The method of calculation and results are given in appendix A.

4.2.1 Mechanism of Heat Transfer

Mechanism of heat transfer can be explained on the basis of cooling curves. A typical cooling curve can be taken from Fig.4.5. From the figure it is observed that the surface temperature of the samples decrease continuously with time. Curve 'A' denotes the change in temperature with time for the surface at r = 0; z = 2.5mm and curve 'a' denotes the surface at r = 0.; z = 41.5 mm. The cooling behaviour for these two surfaces are different. In case of 'A' there is no differential cooling and sample is continuously cooled by mist right from the beginning. But surface denoted by 'a', has differential rate of cooling. The temperature decreases slowly at the higher temperature range (800 - 500°C) and comparatively faster cooling occurs at the lower temperature range.

4.2.2 Initial Temperature

The effect of initial temperature on cooling is given in Fig.4.5 and the corresponding heat transfer coefficient versus surface temperature plot is given in Fig.4.6. From Fig.4.6 it can be seen that for all the initial temperatures, decrease in surface temperature increases the heat transfer coefficient. At constant initial temperature at 800° C ,When surface temperature varies from 600°C to 200°C the h values vary from 50 to 5500 $Wm^{-2}k^{-1}$. When the initial temperature is varied from 600°C to 900°C, then the h value increases with decreasing surface temperature. From Newton's law of cooling,

$$h = \frac{q}{A\ \Delta T} = \frac{k\ A\ (\Delta T/\Delta x)}{A\ \Delta T} \tag{4.3}$$

From the above expression, it can be seen that the increase in h
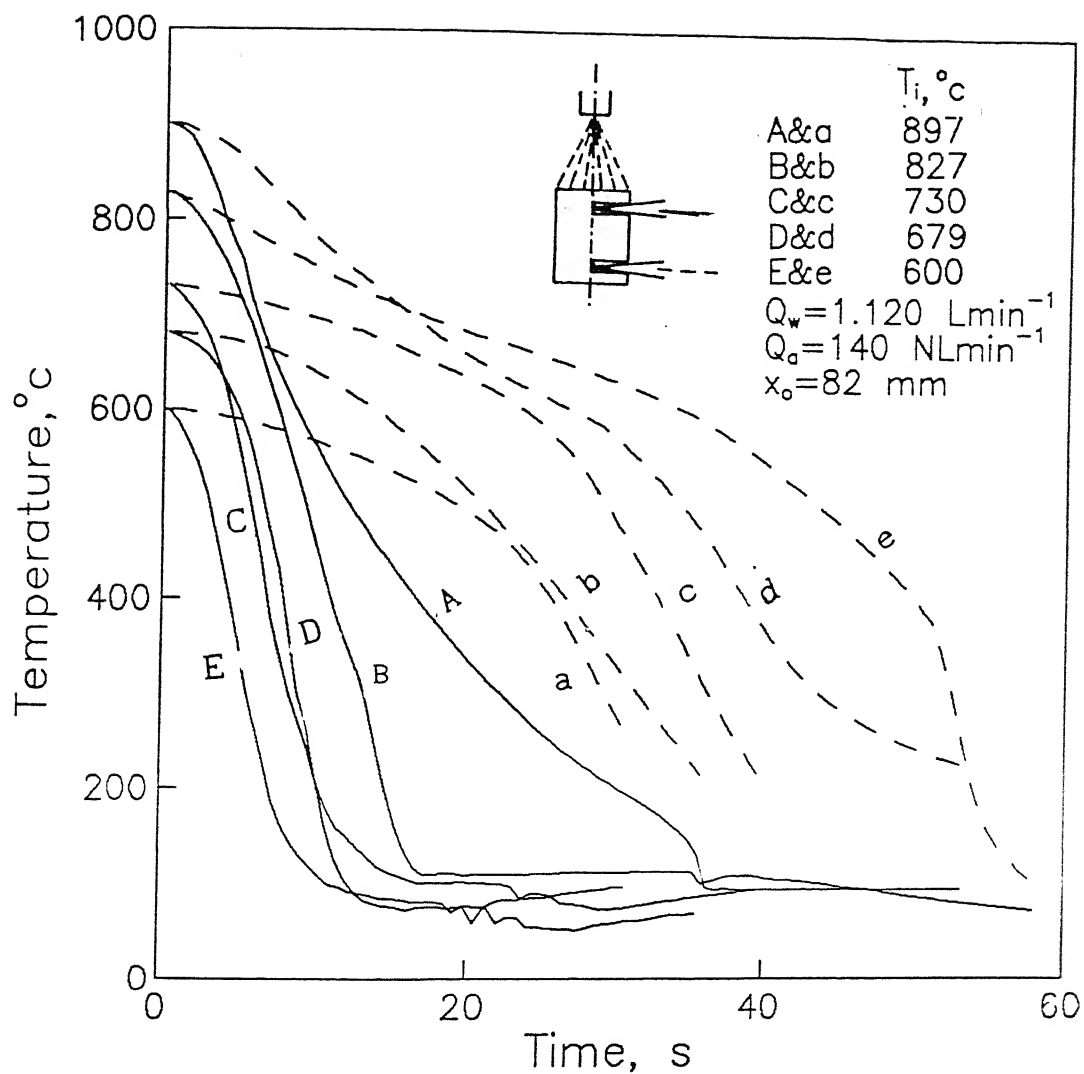
Fig. 4.5 Effect of initial temperature on cooling
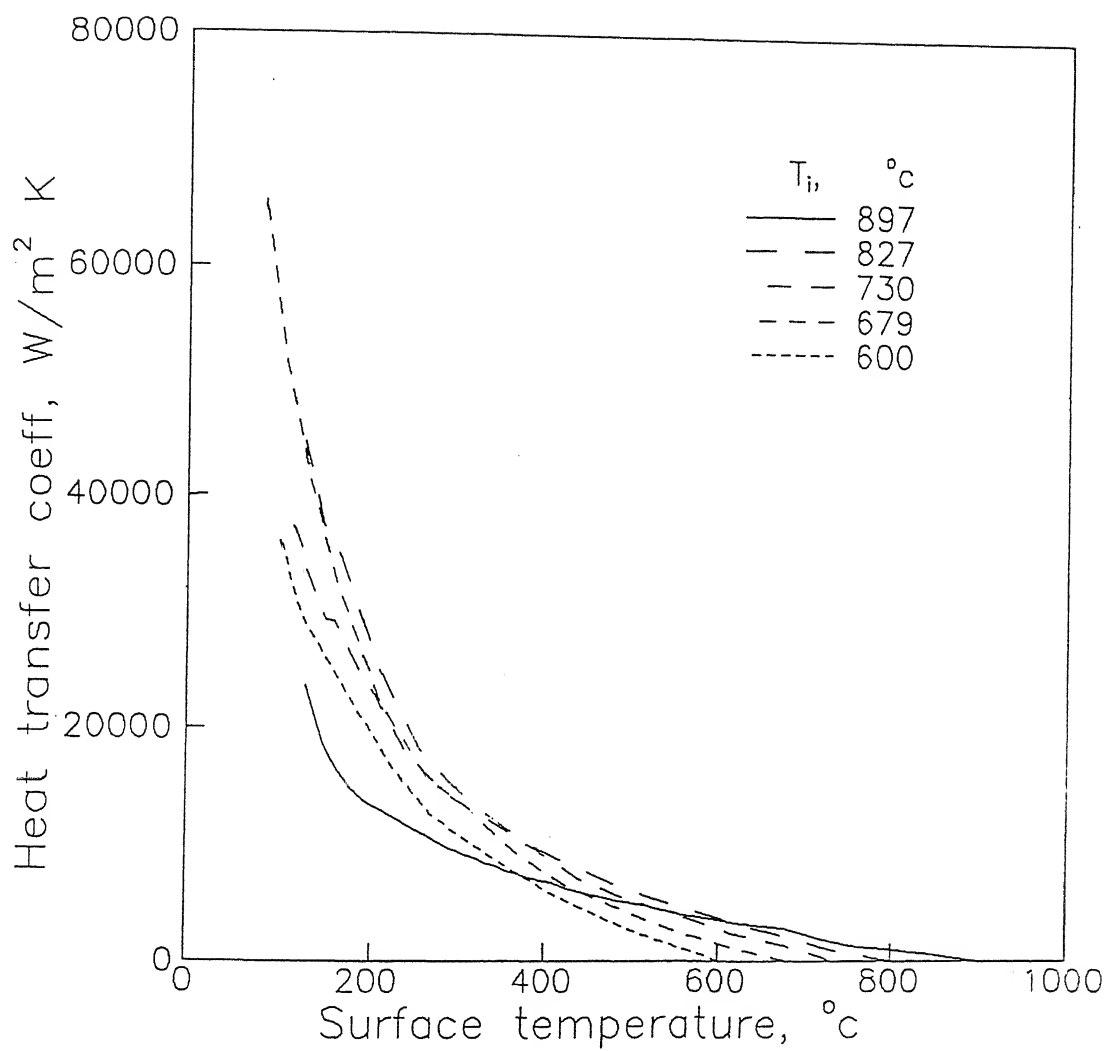
Fig. 4.6   Influence of initial temperature on heat transfer coefficient at different surface temperatures.

value are due to the increase in heat flux and decrease in ΔT during cooling. At higher temperature region $600^{\circ}C$ to $897^{\circ}C$ for all the surface temperatures, increase in T_i increases the h value. Increase in $\delta T/\delta x$ gradient increases the heat flux and thereby increasing the h value. But at lower temperature range (below $600^{\circ}C$) for the increase in T_i decreases the h values. This is due to the decrease in $\delta T/\delta x$ values. At $T_i = 897^{\circ}C$, when T_s varies from $850^{\circ}C$ to $500^{\circ}C$, h value from 600 to 5000 $Wm^{-2}k^{-1}$. These values are in good agreement with the literature [19, 20].

It can be observed from the figure that h_{max} value decreases with increasing T_i. When T_i varied from $680^{\circ}C$ to $897^{\circ}C$, the h_{max} varies from 66000 to 24000 $Wm^{-2}k^{-1}$.

4.2.3 Water Flux

4.2.3.1 Mist Nozzle

From Table 4.4, it can be noticed that the variation in air, water flow rates and spray distance ultimately effects the water flux. So the cooling curves are plotted for the variation in water flux and shown in Fig.4.7. The Fig.4.8 shows the variation of h with surface temperature for different water flux. It is observed that, h increases with decrease in surface temperature for all water flux. But at higher temperature ($600^{\circ}C$ to $800^{\circ}C$), there is no effect of water flux on the heat transfer coefficient. But at lower temperature (less than $600^{\circ}C$), increase water flux slightly increases the h value.

4.2.3.2 Water Spray Nozzle

The effect of water flux on heat transfer is studied for the water spray nozzle and the cooling curve is given in Fig.4.9. Corresponding h versus T_s curve is shown in Fig.4.10. At higher temperature range (600 – $800^{\circ}C$), the same trend is observed here also, as it is in the case of mist

Temperature, °C

1000

800

600

400

200

0

0   20   40   60

Time, s

$\dot{q}_w$ $Lm^{-2}s^{-1}$
A&a   12.22
B&b   32.59
C&c   40.74
D&d   55.00
E&e   63.15
T_i = 827°C

a
b
c
d
e

A
B
C
D
E
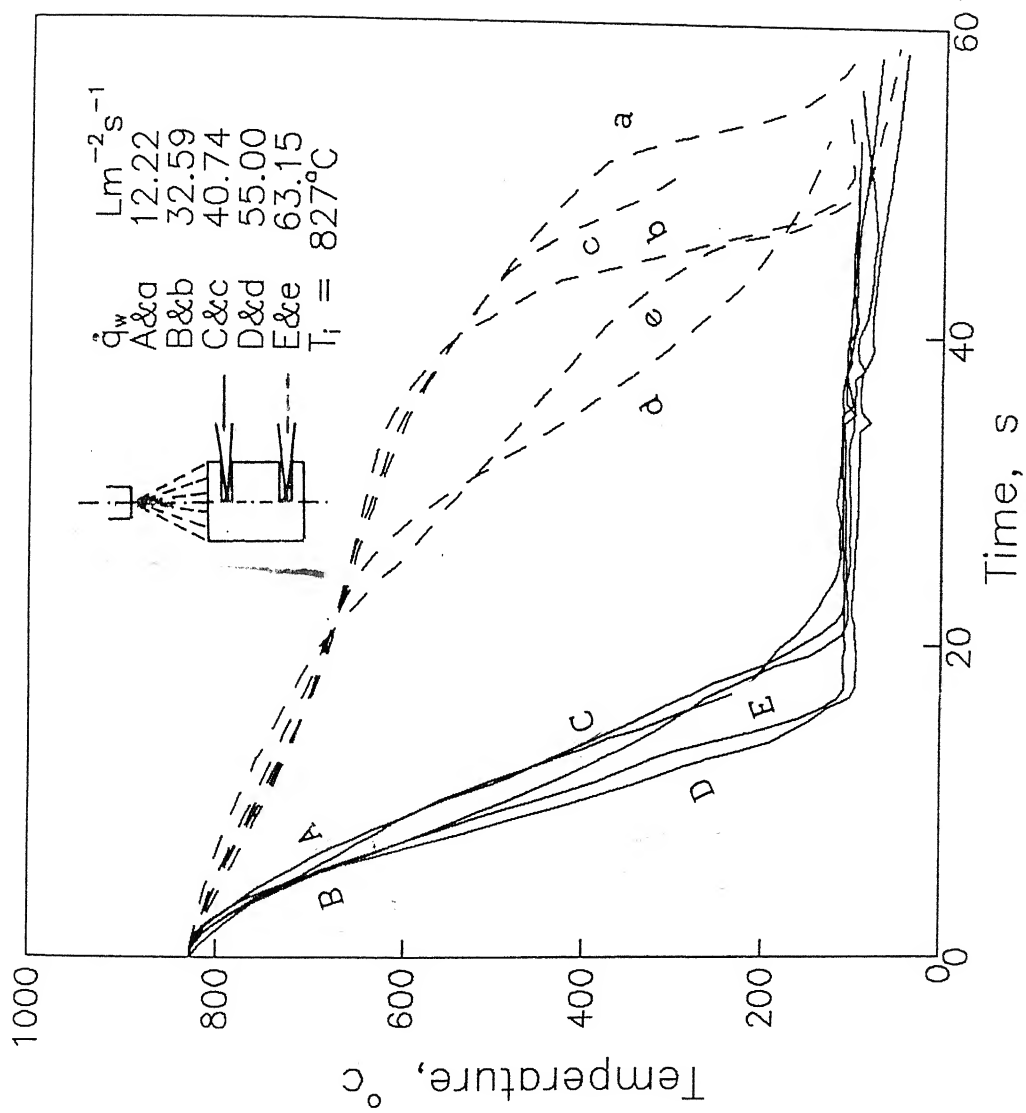
Fig. 4.7   Effect of water flux on cooling
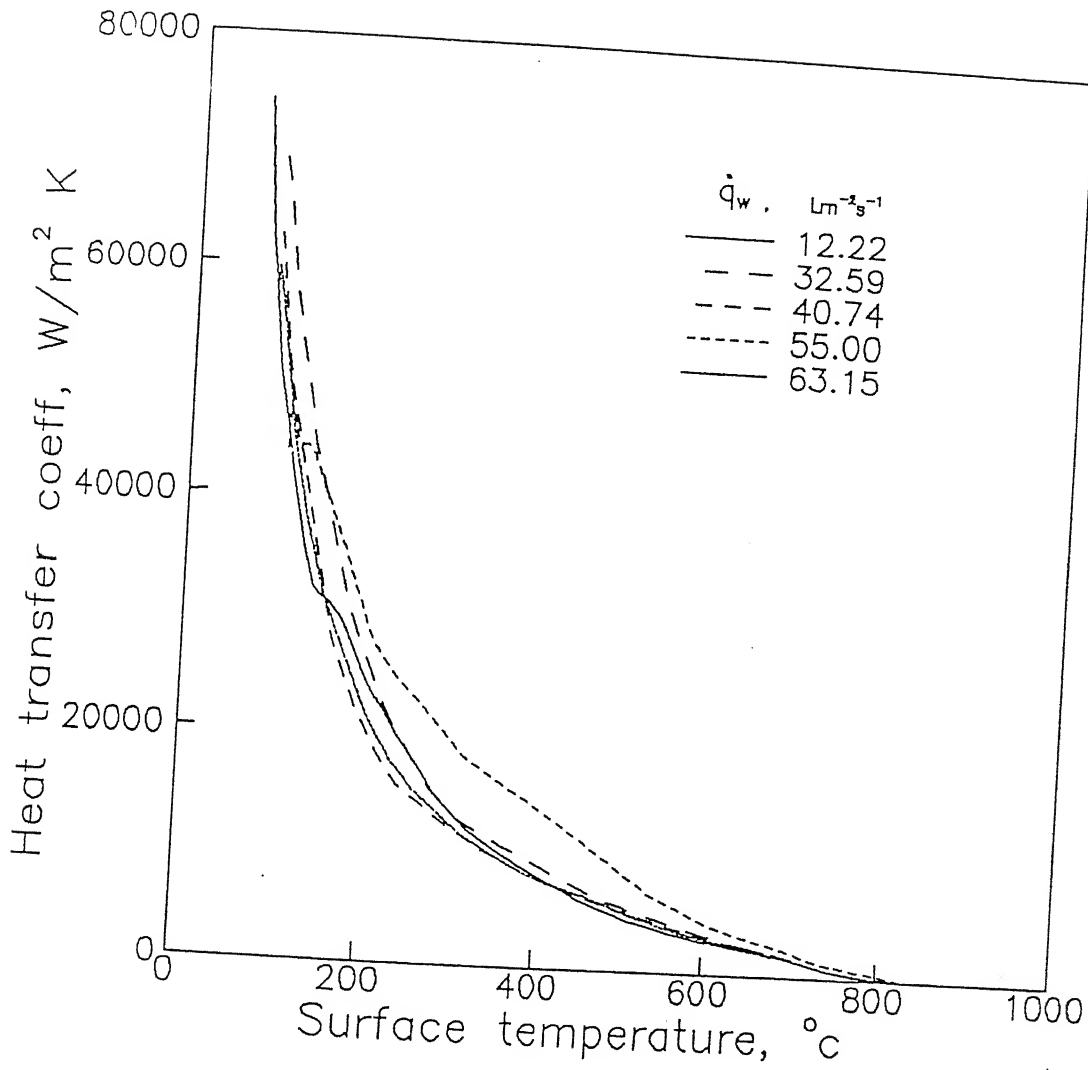
4.8 Influence of water flux on heat transfer coefficient at different surface temperatures.
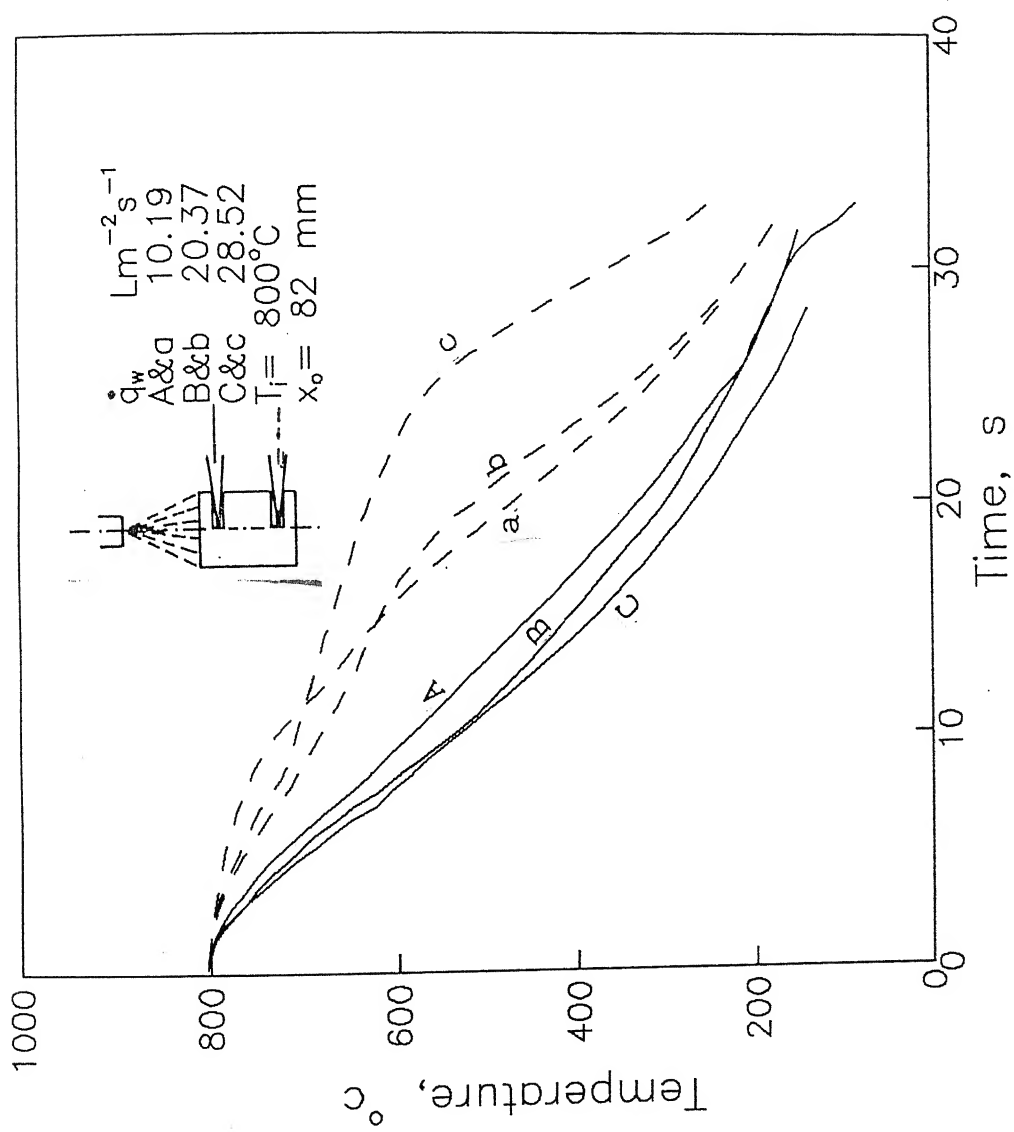
Fig. 4.9 Effect of water flux on cooling for water spray nozzle
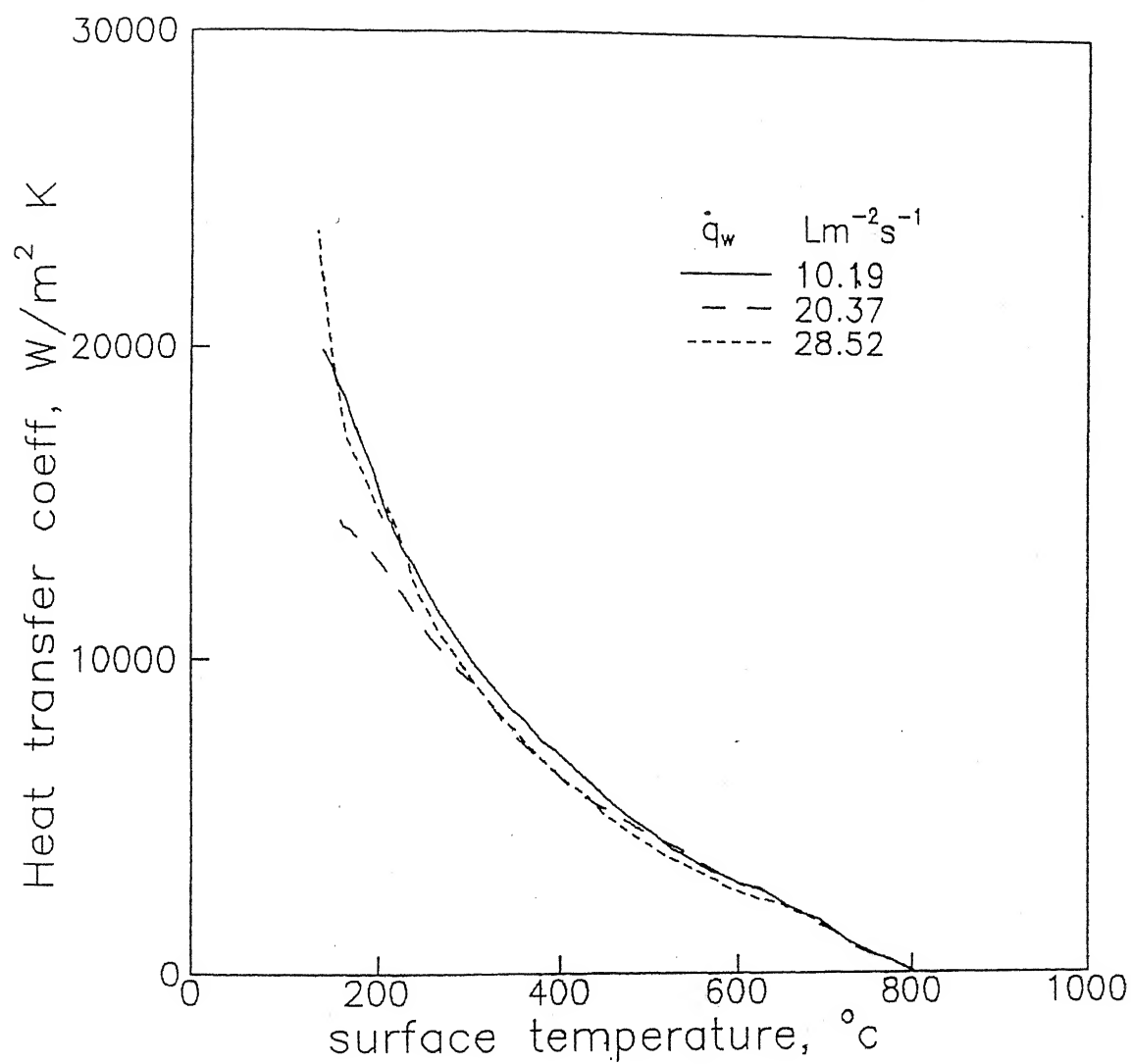
Fig. 4.10 Influence of water flux on heat transfer coefficient at different surface temperature for water spray nozzle.
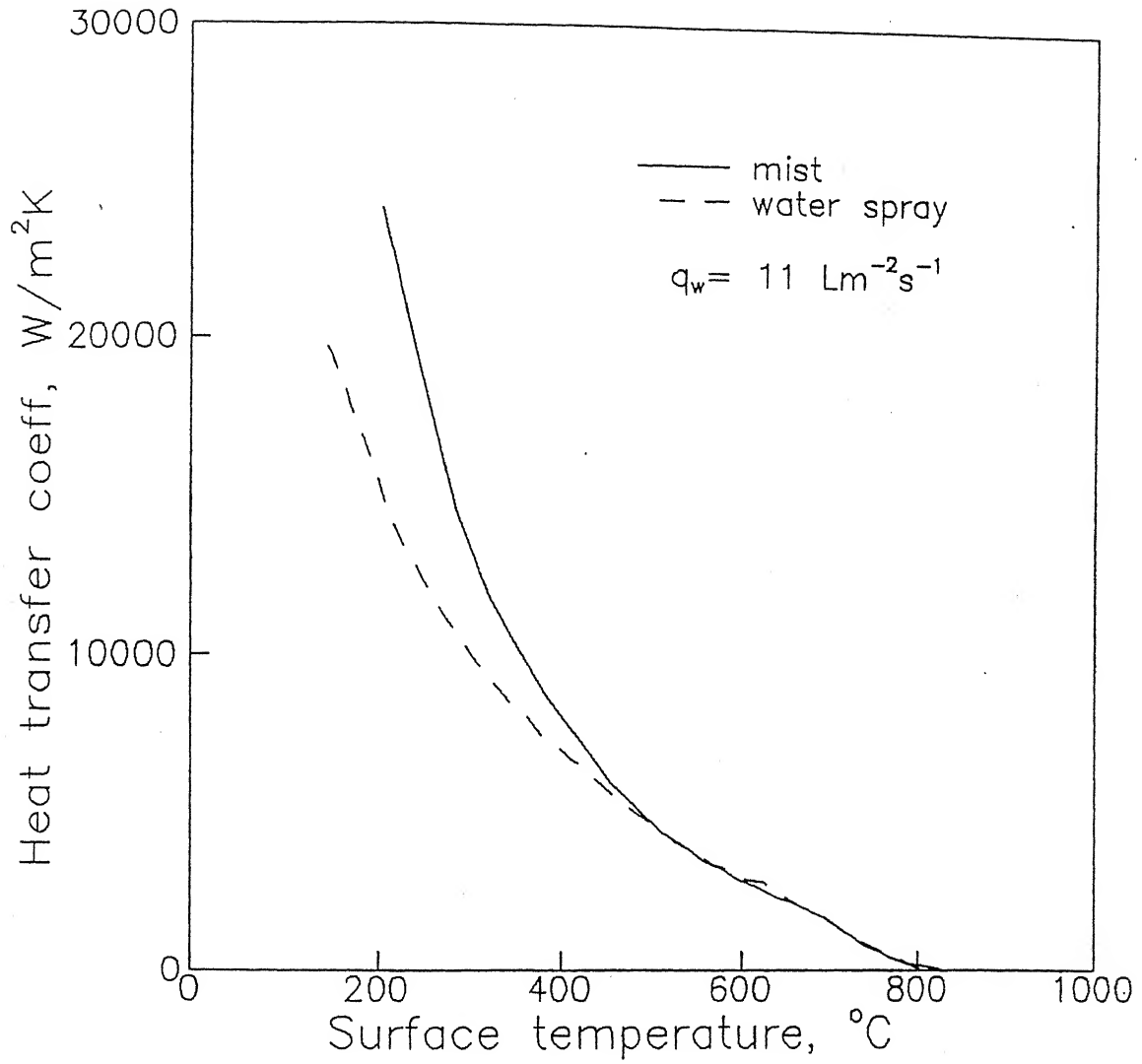
Fig. 4.11 Variation of heat transfer coefficient with surface temperature
for same water flux for both nozzle.

nozzle.

Heat transfer coefficient with surface temperature curve is plotted for the same water flux (around 11 $Lm^{-2}s^{-1}$)for both mist and water spray and is shown in Fig. 4.11. It is noted that for the same water flux in both the sprays, h values are of the same order.

4.2.4 Shielding and Reheating

In the Fig. 4.12, the effect of reheating and shielding on cooling are shown. To get the idea about the effects of sample shape, cylindrical and rectangular samples are used. Corresponding heat transfer coefficient versus surface temperature curve is given in Fig. 4.13. From the figure it is observed that the effects of shielding, reheating and the sample shape on the heat transfer coefficient value at all the surface temperature, are practically negligible. It can be seen from the figure that at temperature 400 - 800°C, the various curves fall on each other.

4.2.5 Themophysical Properties

The effect of thermo physical properties on cooling is given Fig. 4.14. The heat transfer coefficient versus surface temperature curve for the above studies is plotted in Fig.4. 15. The figure shows that h depends on type of metal i.e. thermophysical properties (Thermal conductivity k, density ρ and specific heat C_p). At any surface temperature it is found that h for copper is higher than brass and steel. The higher values of h are due to greater thermal diffusivity of copper as compared to steel and brass.

At higher temperature (600 - 800°C) it is noticed that, variation in carbon content in steel does not affect the heat transfer coefficient values. In literature [21], It is reported that the thermophysical properties will effect h values and h for copper is greater than Ni on the
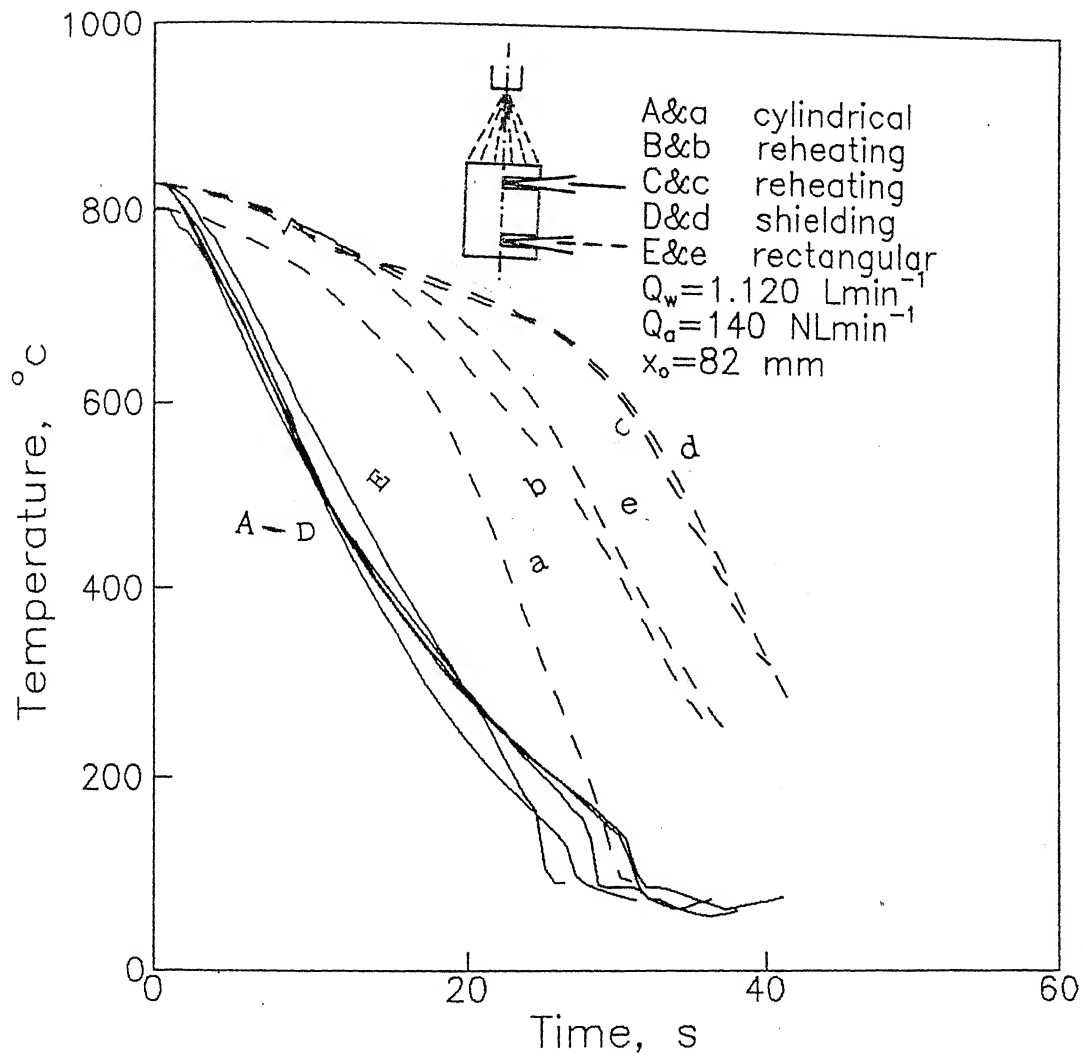
. 4.12 Effect of reheating, sheilding and sample shape (rectangular) on
   cooling.
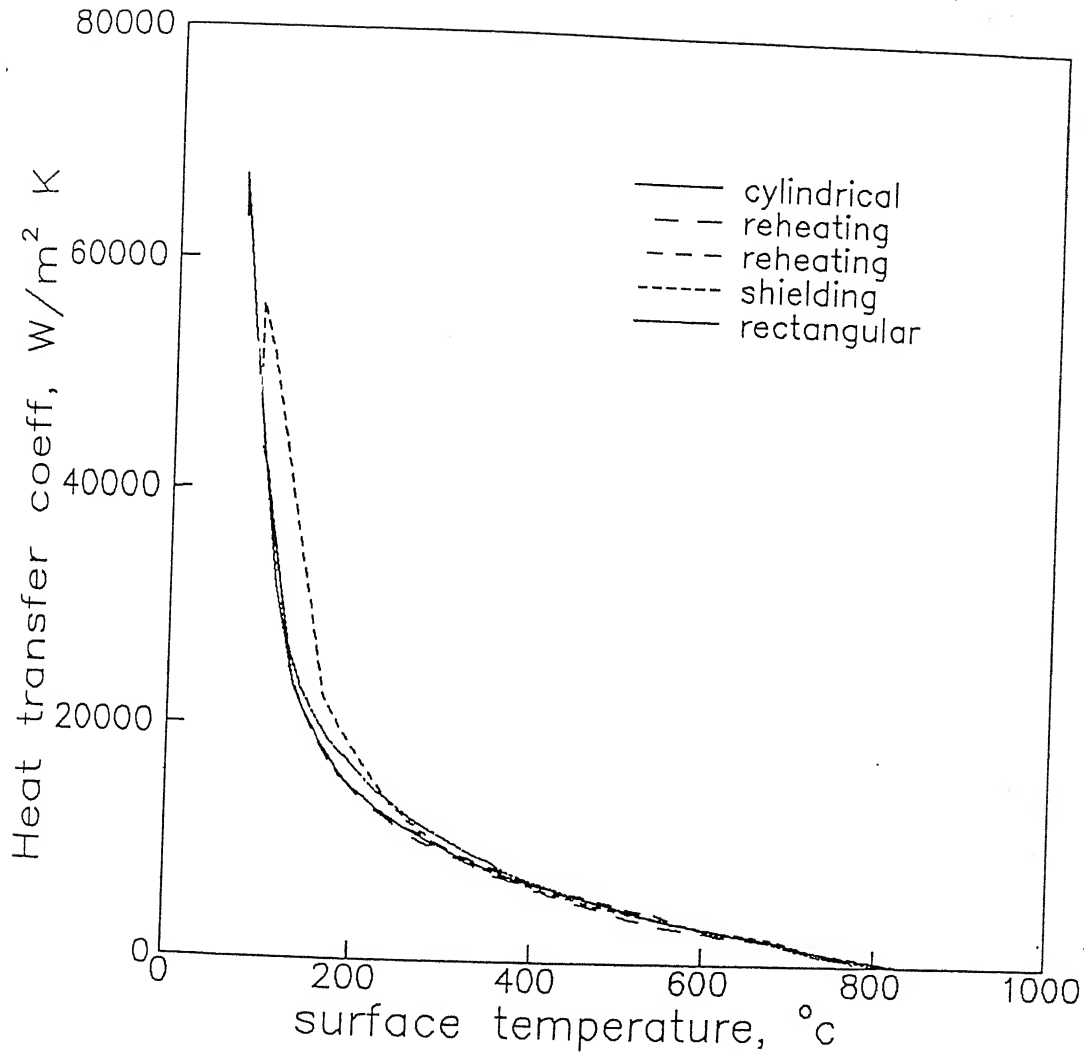
4.13 Influence of reheating, sheilding and sample shape (rectangular) on heat transfer coefficient at different surface temperatures.
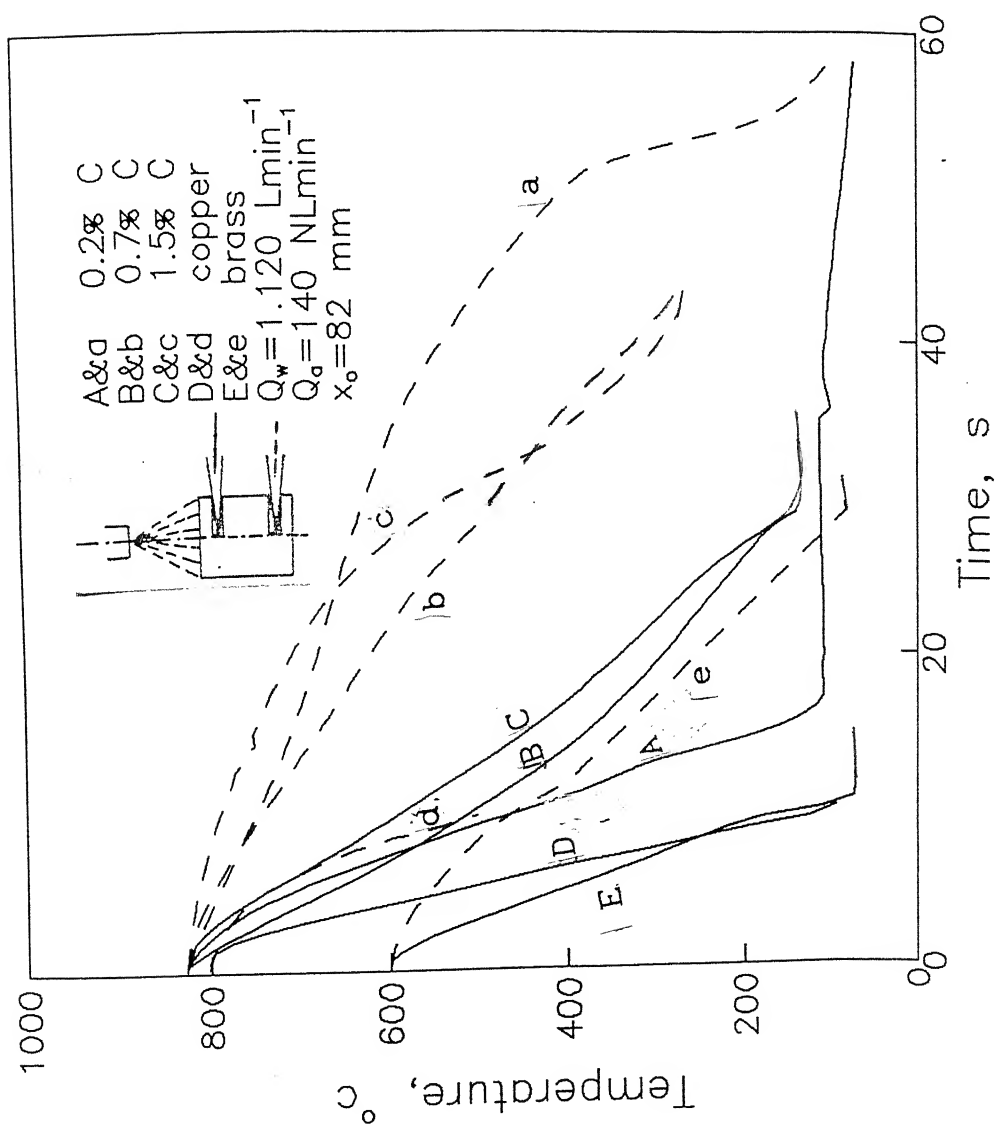
Fig. 4.14 Effect of thermophysical properties on cooling

Legend inside figure:

A&a	0.2%	C
B&b	0.7%	C
C&c	1.5%	C
D&d	copper	
E&e	brass	

$Q_w = 1.120$ $Lmin^{-1}$
$Q_a = 140$ $NLmin^{-1}$
$x_o = 82$ mm

Temperature, °C (vertical axis: 0, 200, 400, 600, 800, 1000)

Time, s (horizontal axis: 0, 20, 40, 60)
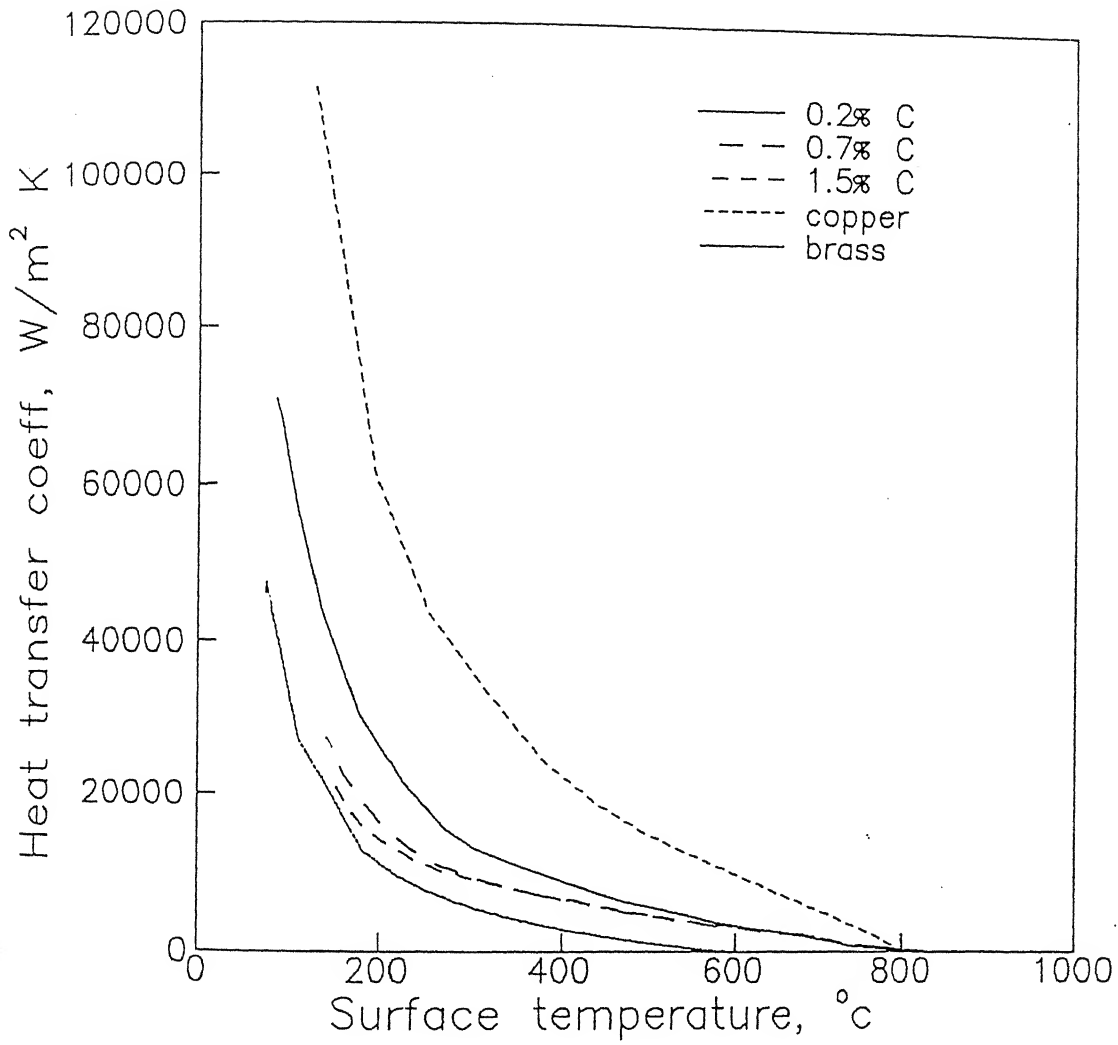
Fig. 4.15 Influence of thermophysical properties on heat transfer

coefficient at different surface temperatures.

entire range of T_s as their thermophysical properties are different.

From the Fig.4.14, it can also be seen that h_{max} value increases with intrusion coefficient $(k \rho C_p)^{0.5}$. When intrusion coefficient increases from 10000 to 37000, then h_{max} value increases from 20000 to 110000 $Wm^{-2}K^{-1}$. This can be explained on the basis of thermal conductivity (k) and specific heat (C_p). For example, at $800^{\circ}C$, for steel samples k = 24.7 $Wm^{-2} K^{-1}$, ρ = 7844 $Kg\ m^{-3}$ and C_p = 605 $KJ\ Kg^{-1}\ K^{-1}$ and for copper samples k = 338 Wm^{-2} K, ρ = 8960 Kgm^{-3} and C_p = 454 $KJ\ Kg^{-1}K^{-1}$. Due to low thermal conductivity and high specific heat steel cools more slowly than copper.

4.2.6 Type of Cooling

Rate of cooling is mainly affected by the type of cooling. The cooling curves are shown in Fig. 4.16. The corresponding heat transfer coefficient versus surface temperature curve is given in Fig. 4.17. The heat transfer coefficient value increases with decrease in surface temperature for all type of cooling. For air cooling, in the whole temperature $(200-800^{\circ}C)$ range, h value lies below 1700 $Wm^{-2}k^{-1}$. In the case of water spray cooling, h value starts increasing right from the beginning of the fall in surface temperature and h_{max} value is of the order of 20000 $Wm^{-2}k^{-1}$. But, mist cooling has more influence in the heat transfer coefficient values. The h value increases slowly with decrease in surface temperature. At lower temperature range, below $400^{\circ}C$, there is a large increase in h value and h_{max} value is around 70000 $Wm^{-2}k^{-1}$.

From the above results, it can be seen that at high T_s $(600-800^{\circ}C)$, there is no effect of water spray or mist cooling on the heat transfer coefficient values. Below $600^{\circ}C$, h_{mist} is greater than $h_{water\ spray}$ for the same amount of water flow rate. In case of the water
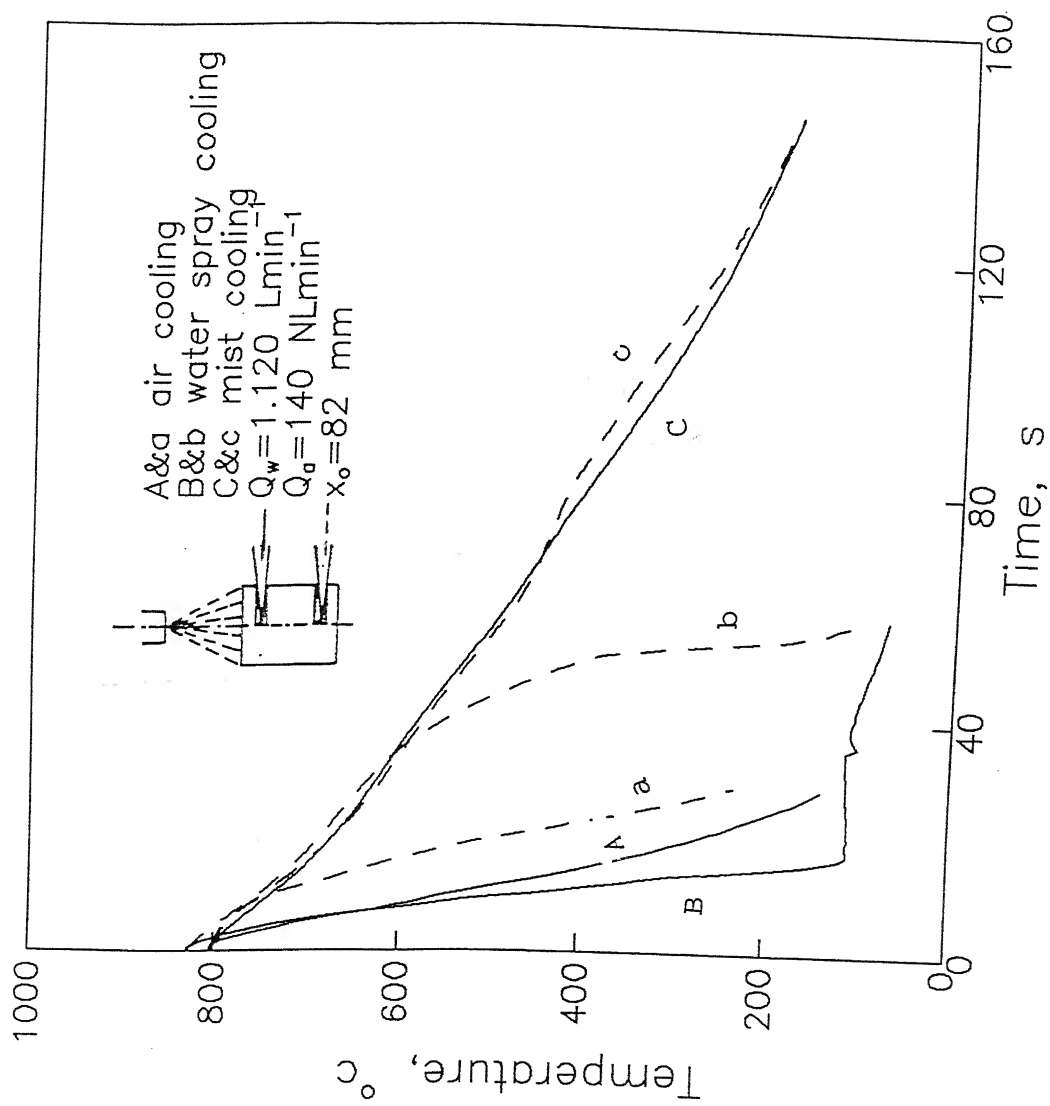
Fig. 4.16 Change of cooling characterstics due to different types of cooling.
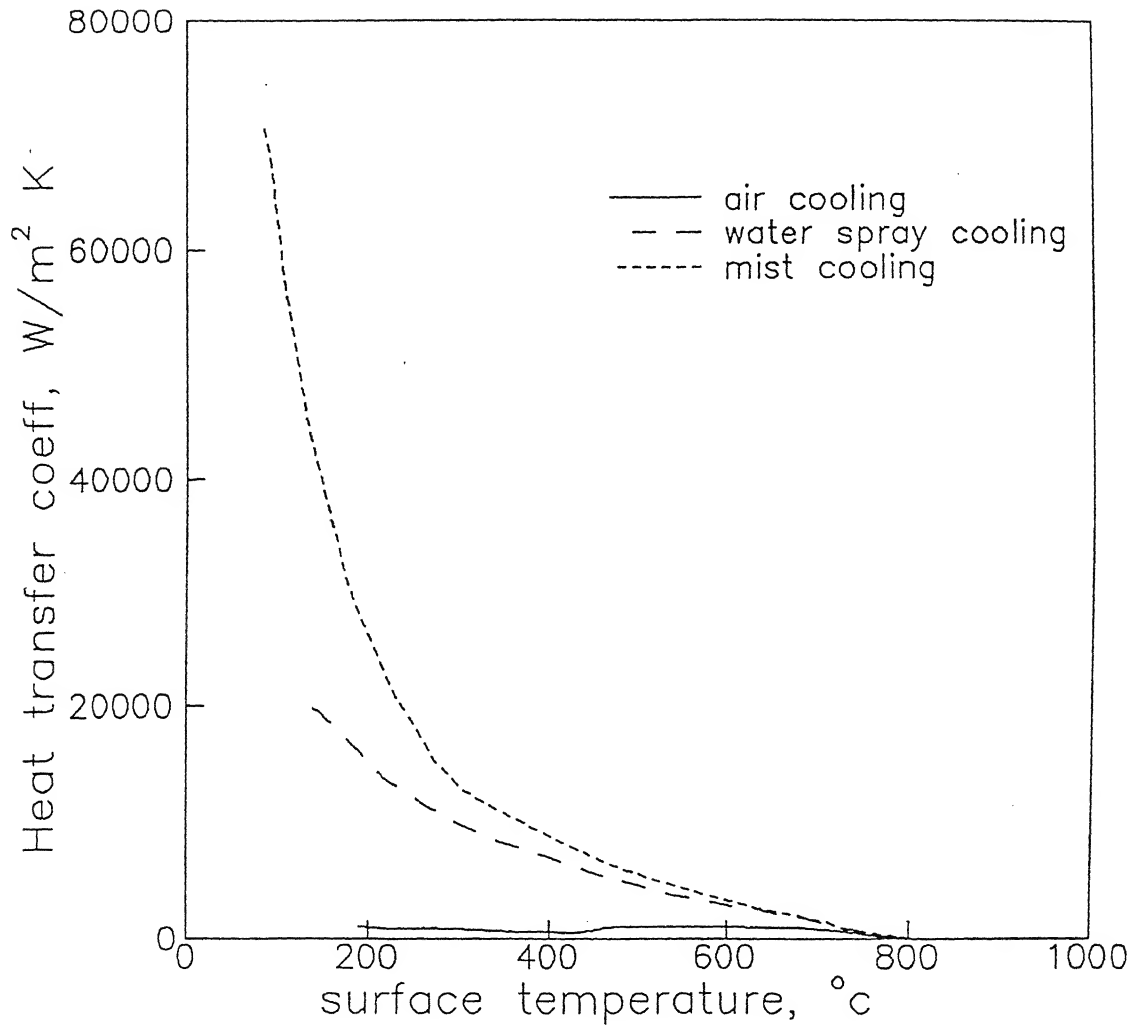
;. 4.17 Effect of different types of cooling on heat transfer coefficient at different surface temperatures.

spray nozzle, water flux is obtained in the range of 12 $Lm^{-2}s^{-1}$ and that for the mist nozzle is around 33 $Lm^{-2}s^{-1}$ for the water flow rate 1.120 $Lmin^{-1}$. From the above water flux values it can be seen that same water flow rate gives higher water flux for mist nozzle and lower water flux in the case of water spray nozzle. To get the same water flux, in case of water spray, the amount of water should be increased to higher values.

4.3 QUENCHING

Plain carbon steel samples are cooled in mist and water spray after heating up to $800^{o}C$. The samples are also directly quenched in water. Then the samples are observed under the optical microscope. Hardness values are measured at various depths from the cooling end ($r = 0$ and z varies from 1 mm to 44 mm) for all the samples and found to be R_c values varies from 54 to 42. Fig. 4.18 shows the variation in hardness with distance from cooling end. Hardness measurement is also done in radial direction ($z = 0$; when r is varied from 0 to 12.5 mm) and in this case R_c varies from 54 to 49.5. The hardness values are in total agreement with the water cooled sample also. For the water quenched sample at $r = 0$. and z varying from 1mm to 41mm the hardness is 52 R_c.

Fig. 4.19 reveals the microstructure of the plain carbon steels observed with optical microscope. At various depth from the cooling end the photographs are taken. For the plan carbon steel, martensite is formed in the cooling end and pearlite + ferrite in the next end. From [26] it is observed that the hardness values obtained in the present study are in good agreement with the literature values. Due to quenching, formation of martensite is observed through out the sample.
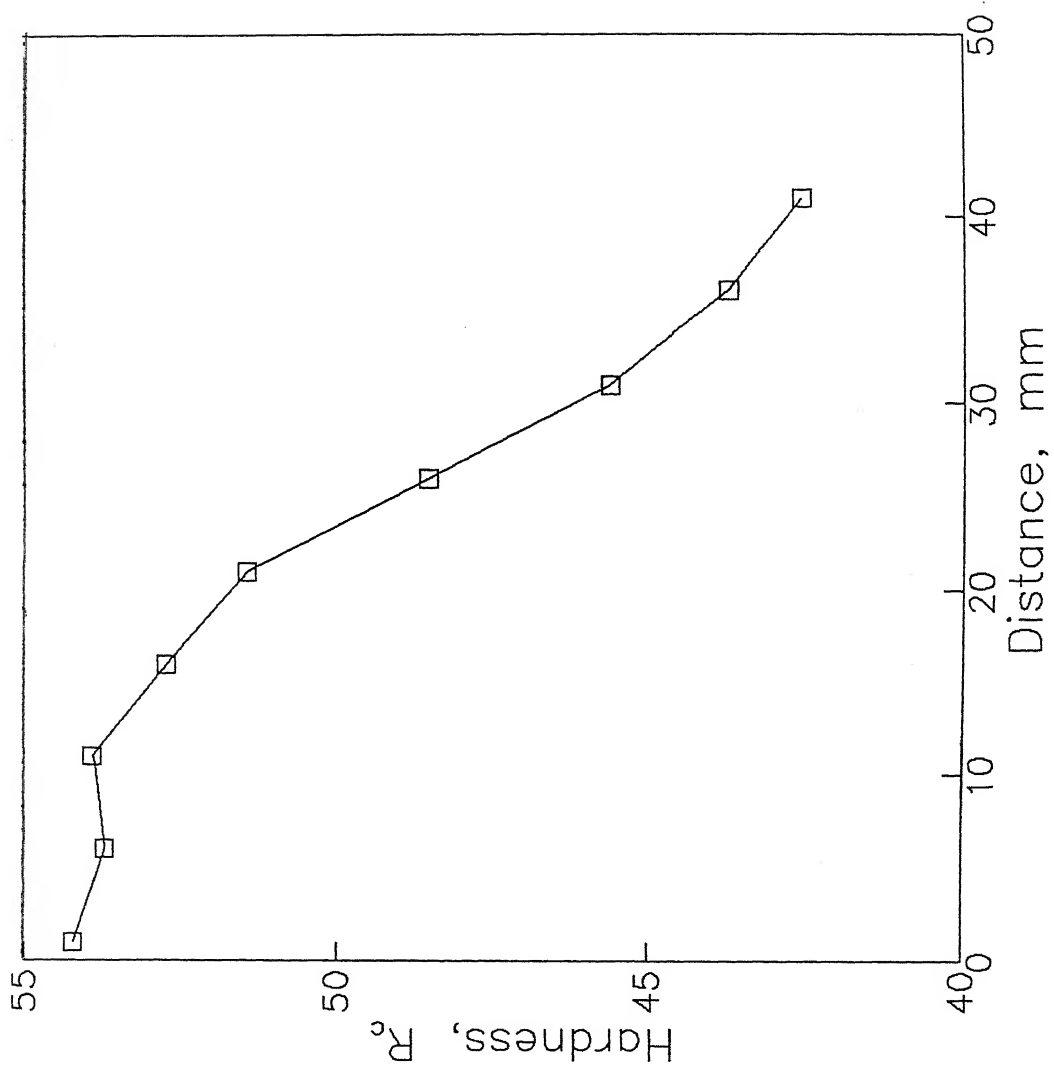
Fig. 4.18 Variation of hardness with distance from the cooling end.

CHAPTER 5

CONCLUSIONS

The characterisation of mist and water spray nozzles and their heat extraction capabilities are emphasized in this work. The major outcomes of the study are enlisted below.

1) Pressure drop in the mist nozzle is greater than that in water spray nozzle at any given water flow rate.

2) There is no effect of water flow rate on the variation of air pressure in the air flow rate.

3) Water and air flow rate affect the structure of two phase jet. At various combination of air and water flow rates, different regions in the two phase jet are observed, namely, 1) partial water 2) coarse mist 3) mist 4) pulsation. In mist region, the two phase jet is observed to have many fine droplets of water moving in air. To get mist, optimum values of air and water flow rate must be maintained.

4) Water flux increases with increase in water flow rate, decrease in air flow rate and decrease in spray distance. There is large effect of spray distance on water flux when compared to water air flow rate.

5) Heat transfer measurements are similar to pool boiling and decrease in surface temperature increases the heat transfer coefficient. At higher temperature range, there is no effect of water flux, initial temperature and carbon content of steel on heat transfer coefficient. Thermophysical properties affects the heat transfer coefficient at any surface temperature, $h_{copper} > h_{brass} > h_{steel}$ for the same water flux. At the same water flow rate, $h_{mist} > h_{water\ spray}$ where as at same water flux $h_{mist} \simeq h_{water\ spray}$.

CHAPTER 6

SUGGESTIONS FOR FUTURE WORK

1. In the present study, the structure of two phase mixture is observed visually. Measurement of droplet size by photographic technique will give better explanation of structure of two phase flow.

2. Heat transfer studies are carried out for the cylindrical and rectangular specimens. Similar kind of studies can be performed for steel plates also.

3. Two thermocouples are fixed at two positions in the sample. More number of thermocouples can be used for more accurate values of the heat transfer coefficient.

4. Initial temperature of the sample can be increased above $1000^\circ C$ for the calculation of heat transfer coefficient.

5. The water flux values considered in the present investigation are very large. Due to the high water flux values, the wetting behaviour could not observed clearly. To observe the wetting behaviour, studies can be made by considering lower water flux values.

6. Only one nozzle is used in the present study. Two or more nozzles can be used to cool the specimen and the overlapping behaviour of the sprays can be studied.

References

1) Koria, S.C. and Mehrotra, S.P. Short term course on continuous casting of steel (1991).

2) Nakamura, O.; Mitsuksuka, M; Suenaga, K. and Kimishima, K. Trans ISIJ, 25, 1985, pp 475 - 482.

3) Mitsuksuka, M. and Fakuda, K. Trans. ISIJ, 21, 1986, pp 689 - 698.

4) Koria, S.C. and Datta, I. Steel Research 63, 199, pp 19 - 26.

5) Mitsuksuka, M; Morise, H; Ogura, T. and Nakamura, O. Trans ISIJ, 25, 1985, pp 467 -474.

6) Yoshimura, M; Suzuki, S; Chielense, A. and Benott, P. In continuous casting 85, Proc. International Conference, Iron making and Steelmaking committee of the Institute of Metals, London. 22 - 24 May 1985, paper no. 21.

7) Grothe, H.; Rdot, J.P.; Shima, T.; Watters, J.; Willium, F. and Wolf, M. In continuous casting 85, Proc. International Conference, Iron making and Steelmaking committee of the Institute of Metals, London. 22 - 24 May 1985, paper no. 68.

8) Misuksuka, M.; Fukuhisa, Y.; Wake, M.; Okajima, M.; Miyashita, N. and Takeda, Y. Trans ISIJ, 25, 1985, pp 1244 - 1250.

9) Yanagi, K. Mitsibushi Iukoguno, 9, 1972, pp 792

10) Mizikar, E.A. Iron and Steel Engineer, 1970, pp 53 - 60.

11) Pederson, C.O. Int. J. of Heat and Mass Transfer, 1970, pp 369.

12) Akao, F.; Araki, K.; Mori, S. and Moriyam, A. Trans ISIJ, 20, 1980, pp 737 - 743.

13) Savic, P. and Bault, G.J. Nat. Res. Lab., Canada Rep. MT.26, 1955.

14) Wachters, L.H.J. and Westerling N.A.J. Chem. Engg. Sci., 21, 1966, pp

1643.

15) Narasaki, S.; Miyashita, N.; Doki, M. and Abe, Y. Trans ISIJ, 24, 1984, pp B78 - B79.

16) Hoogendorn, C.J. 5th Int. Heat Transfer Conf. paper organized by Science Council of Japan IV 1974, pp 135.

17) Brimacomb, J.K.; Agarwal, P.K.; Hibbins, S.; Prabhakar, B. and Baptista, L.A. Continuous Casting Vol 2, Iron and Steel Society of AIME, 1984, pp 109 - 123.

18) Brimacomb, J.K.; and Soumachi, K., Met Trans B, 88, 1977, pp 489.

19) Jescher, R. and Miiller Arch. Eisenhuttnmes, 44, 1973, pp 589 - 594.

20) Kumoika, N. Tetsu - to - Hagne, 64, 1978, pp 5255.

21) Jeschr, R.; Reiners, U. and Scholz, R. Steelmaking Proceedings, 69, 1986, Washington D.C. pp 511 - 521.

22) Bolle, E. and Mourean, J.C. Proceedings of two phase flow of heat transfer, Vol II, NATO Advanced Study Institute, 1978, pp 1327.

23) Bolle, E. and Mourean, J.C. Int. Con. on heat and mass transfer in metallurgical process, Yugoslavia, 1979.

24) Kohler, C.; Jescher, R.; Scholz, R.; Slowik, J. and Borchart, G. Steel Research 61, 1990, No.7, pp 295 - 301.

25) Reiners, U.; Jescher, R.; Scholz, R.; Zebrowski, D. and Reiht, W. Steel Research 56, 1985, No.5, pp 239 - 246.

26) Avner, A.H. Introduction of Physical Metallurgy, McGrowhill publication.

27) Koria, S.C. and Datta, I. Ironmaking and Steelmaking 19, 1992, pp 394 - 401.

APPENDIX A

NUMERICAL SOLUTION FOR THE CALCULATION OF HEAT TRANSFER COEFFICIENT

Assuming a one-dimensional unsteady state heat transfer, the temperature distribution in the test piece is expressed by the fundamental equation

$$\frac{\partial T}{\partial t} = \frac{k}{\rho \, C_P} \frac{\partial^2 T}{\partial x^2} \tag{A1}$$

Initial condition:

$$T(x, \, 0) = T_o \tag{A2}$$

Boundary conditions

$$T(0, \, t) = f(t) \tag{A3.1}$$

$$T(L, \, t) = f^{'}(t) \tag{A3.2}$$

Based on the calculated inner temperature of test piece, heat transfer coefficient 'h' was obtained from the eq

$$t > 0 \, : \; \left. \frac{\partial T}{\partial x} \right|_{x=0} = -\frac{h}{k} \, (T - T_w) \tag{A4}$$

where x is co-ordinate.

Finite Element Method (FEM) was employed to solve the Fourier differential Eq. (A1) with its initial and boundary conditions. To find the heat transfer coefficient at a point in a specimen at some temperature T one needs to calculate $\frac{\partial T}{\partial x}$ at that point.

$$\frac{\partial T}{\partial x} \approx \lim_{x_1 \to x_2} \frac{T_2 - T_1}{x_2 - x_1}$$

$$\text{i.e.,} \; \frac{\partial T}{\partial x} \approx \lim_{x_1 \to x_2 \to 0} \frac{T_2 - T_1}{x_2 - x_1} \tag{A5}$$

Thus one needs to have temperature at two points in close

vicinity. The FEM allows to find such temperature grid (Temperature vs time scale).
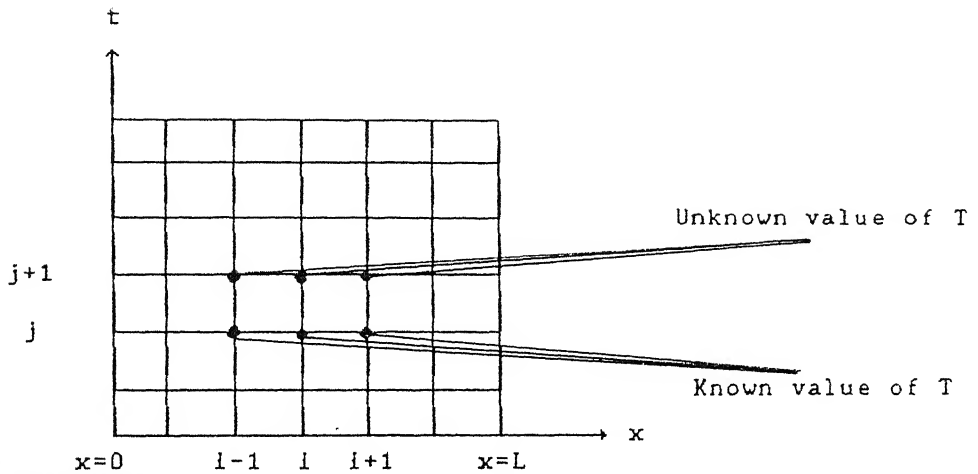
FEM solution for one dimensional transient heat conduction equation

Governing differential equation

$$\frac{\partial T}{\partial t} - \frac{\partial}{\partial x} \left(\frac{k}{\rho C_P} \cdot \frac{\partial T}{\partial x} \right) = 0 \tag{A1}$$

Application of Galerkin method on Eq. (A1) results in the elemental equation

$$[C] \{\dot{T}\}^n + [k_T] \{T\}^n = \{p\}^n \tag{A6}$$

where $[C] = \dfrac{\partial x}{6} \begin{bmatrix} 2 & 1 \\ 1 & 2 \end{bmatrix}$

$$[k_T] = \frac{k}{\rho C_P} \frac{1}{\Delta x} \begin{bmatrix} 1 & -1 \\ -1 & 1 \end{bmatrix}$$

Δx is element length.

Implicit scheme dictates that,

$$\left. \begin{aligned} \{\dot{T}\}^n &= \frac{\{T\}^n_{p+1} - \{T\}^n_p}{\Delta T} \\ \{T\}^n &= \{T\}^n_{p+1} \\ \{p\}^n &= \{p\}^n_{p+1} \end{aligned} \right\} \tag{A7}$$

where subscript p indicate the previous time and p+1 is the present time and Δt is the time step and n indicates nodes.

The substitution of Eq.(A7) in Eq.(A6) results

$$\left(\frac{1}{\Delta T} \ [C] \ + \ [k_T] \right) \ \{T\}^n_{p+1} \ = \ \{p\}^n_{p+1} \ + \ \frac{1}{\Delta t} \ [C] \ \{T\}_p \qquad (A8)$$

Thus for each element Eq. (A8) has been applied and ultimately all the elemental equations are assembled to obtain global matrix. Eq. (A1) is second order in dimension x and first order in time t. Therefore two boundary conditions and on initial condition are required to solve the resulting global matrix.

Initial condition

At t = 0 $T_p = T_o$

Boundary conditions

At x = 0 $T = T_x = 0$

x = L $T = T_{x=L}$

L is length (of the sample) to interest. Elimination method is used to solve the global matrix with the given boundary and initial conditions. {p} contains the term $\left. \frac{\partial T}{\partial x} \right|_{x=0}$ and $\left. \frac{\partial T}{\partial x} \right|_{x=L}$. Thus with the known temperature at all the nodes $\frac{\partial T}{\partial x}$ at the desired end can directly be obtained from the global matrix and thus heat transfer coefficient can be evaluated.

In Table A1, Code number of Samples used in Table A2 are given, and calculated heat transfer coefficients are given in Table A2

Table A1 Code number samples used in Table A2.

Type of Samples	Variables	Type of Cooling	Code Number
Steel	Initial temperature	Mist	Steel 1-5
	Water flux		Steel 6-9
	Carbon content		Steel 10-11
	Reheating, Shielding & Sample shape		Steel 12-14
Steel	Water flux	Water spray	Steel 15-17
	Carbon content		Steel 18-19
Steel	——	Air	Steel 20
Copper	Water flux	Mist	Copper 1-3
	——	Water spray	Copper 4
	——	Air	Copper 5
Brass	Water flux	Mist	Brass 1-3

```
/*------------------------------------------------------------------------*/
/*                             PREAMBLE                                  */
/*------------------------------------------------------------------------
```

This is one dimensional FEM program for transient heat conduction
equation. It needs two boundary conditions and one initial condition because
of second order derivative with respect to X and first order derivative with
respect to time.

Number of nodes in length direction should not be more than 100
because of memory limitation. In time direction there is no limitation on
the number of nodes. For this particular mist-quenching application 50 nodes
in length direction are enough.

Care must be taken in input data file preparations. The format
of input datafile is (It is assumed that the data is acquired through
interface card)

[channel no.]   [Time of data acquisition]   [milli-volts]   [Temp.]

Prepare seperate data files for cooling-end and the other end.
The present program, in its form, is applicable to steels only. For any
other material changes must be done in
        -> rho
        -> VALUECp
        -> VALUEk
```
------------------------------------------------------------------------*/

#include <stdlib.h>
#include <stdio.h>
#include <math.h>
#include <string.h>


#define MAX_SIZE           100
#define rho_steel          7844.0
#define rho_cu             8940.0
#define rho_brass          8522.0
void nrerror(char *error_text);

#include "ludec.h"          /* ludec.h is the header file containing routines
                               for matrix-invers and matrix-multiplication  */
        int mater;
int main(void)
{
        int ndt = 1,nodxs,nodts,ndx,i,j,ch,sc_ht,sc_wt;
        double Tc,Th,Tw,length,dx,dt,tm,mv,dum,h,dum1,rho;
        double *T_prev[MAX_SIZE],*T_pres[MAX_SIZE],*rhs[MAX_SIZE];
        double *lhs[MAX_SIZE],*lhs_inv[MAX_SIZE];
        char file1[19],file2[19],outf[19];
        FILE *ifp,*ffp,*ofp,*fopen();

        double VALUEk(double T);
        double VALUECp(double T);

        printf("MATERIAL ( 1 for steel, 2 for Cu, 3 for Brass(70-30)) ? ");
        scanf("%d",&mater);

        if (mater == 1) rho = rho_steel;
        else if (mater == 2) rho = rho_cu;
        else if (mater == 3) rho = rho_brass;

        printf("INPUT TEMP. DATA FILE NAME FOR COOLING END ?");
        scanf("%s",file1);
        printf("INPUT TEMP. DATA FILE NAME FOR SECOND END ?");
        scanf("%s",file2);
        printf("OUTPUT FILE FOR HEAT TRANSFER COEFF. ? ");
        scanf("%s",outf);
```

```c
        if (strlen(file1) > 18 || strlen(file2) > 18 || strlen(outf) > 18)
                nrerror("file name should not be more than 20 characters");
        if ((ifp = fopen(file1,"r")) == NULL)
                nrerror("FILE OPENING IS FAILED");
        if ((ffp = fopen(file2,"r")) == NULL)
                nrerror("FILE OPENING IS FAILED");
        if ((ofp = fopen(outf,"w")) == NULL)
                nrerror("FILE OPENING IS FAILED");

        printf("DISTANCE BETWEEN END POINTS (metre) ?");
        scanf("%lf",&length);
        printf("NUMBER OF NODES IN LENGTH AXIS DIRECTION ? ");
        scanf("%d",&nodxs);
        ndx = nodxs-2;   /* substract two boundary nodes from total nodes */
/*-------------------------------------------------------------------------*/
/*                          MEMORY ALLOCATION                              */
/*-------------------------------------------------------------------------*/
        for (i = 0; i <= nodxs-1; i++)
        if ((T_prev[i] = (double *) malloc(sizeof(double))) == NULL)
                nrerror("MEMORY INSUFFICIENT");
        for (i = 0; i <= ndx-1; i++) {
        if ((T_pres[i] = (double *) malloc(sizeof(double))) == NULL)
                nrerror("MEMORY INSUFFICIENT");
        if ((rhs[i] = (double *) malloc(sizeof(double))) == NULL)
                nrerror("MEMORY INSUFFICIENT");
        if ((lhs[i] = (double *) malloc(ndx*sizeof(double))) == NULL)
                nrerror("MEMORY INSUFFICIENT");
        if ((lhs_inv[i] = (double *) malloc(ndx*sizeof(double))) == NULL)
                nrerror("MEMORY INSUFFICIENT"); }
/*-------------------------------------------------------------------------*/

        printf("NUMBER OF NODES IN TIME AXIS DIRECTION ? ");
        scanf("%d",&nodts);
        printf("TIME INTERVAL (sec) ? ");
        scanf("%lf",&dt);
        printf("WATER TEMP (Tw : deg C) ? ");
        scanf("%lf",&Tw);
        dx = length/(nodxs-1);

/*      INITIAL CONDITION         */

        if (!(fscanf(ifp,"%d %f %f %lf",&ch,&tm,&mv,&Tc)))
                nrerror("scanf is failed");
        if (!(fscanf(ffp,"%d %f %f %lf",&ch,&tm,&mv,&Th)))
                nrerror("scanf is failed");

        if (fabs((Tc-Th)/Th)*100.0 > 1.0)
                nrerror("ERROR IN THE INITIAL CONDITION");

        for (i = 0; i <= nodxs-1; i++) T_prev[i][0] = Tc;

        fprintf(ofp,"0.0\t%lf\t%lf\t0.0\n",Tc,Th);

        do {
        printf("PROCESSING NODE IN TIME AXIS :   %d\n",ndt+1);
/*      RHS MATRIX FORMULATION   */

        for (i = 0; i <= ndx-1; i++)
                rhs[i][0] = ((T_prev[i][0]+T_prev[i+2][0])+4.0*\
                                        T_prev[i+1][0])*dx/(6.0*dt);

/*      BOUNDARY CONDITIONS       */

        if (!(fscanf(ifp,"%d %f %f %lf",&ch,&tm,&mv,&Tc)))
                nrerror("scanf is failed");
```

```c
        if (!(fscanf(ffp,"%d %f %f %lf",&ch,&tm,&mv,&Th)))
                nrerror("scanf is failed");

        rhs[0][0]   -= (dx/(6.0*dt)-VALUEk(T_prev[1][0])/(rho*\
                                        VALUECp(T_prev[1][0])*dx))*Tc;
        rhs[ndx-1][0]  -= (dx/(6.0*dt)-VALUEk(T_prev[ndx][0])/(rho*\
                                        VALUECp(T_prev[ndx][0])*dx))*Th;

/*      LHS MATRIX FORMULATION  */

        for (i = 0; i <= ndx-1; i++)
        for (j = 0; j <= ndx-1; j++)
        lhs[i][j] = 0.0;

        for (i = 1; i <= ndx-2; i++)
        for (j = i-1; j <= i+1; j++)
        lhs[i][j] = ((j == i) ? 4.0:1.0)*dx/(6.0*dt)+((j == i) ? \
                        2.0:-1.0)*VALUEk(T_prev[i+1][0])/(rho*dx*\
                                        VALUECp(T_prev[i+1][0]));
        lhs[0][0] = 4.0*dx/(6.0*dt)+2.0*VALUEk(T_prev[1][0])/(rho*dx*\
                                        VALUECp(T_prev[1][0]));
        lhs[0][1] = dx/(6.0*dt)-VALUEk(T_prev[1][0])/(rho*dx*\
                                        VALUECp(T_prev[1][0]));
        lhs[ndx-1][ndx-2] = dx/(6.0*dt)-VALUEk(T_prev[ndx][0])/(rho*dx*\
                                        VALUECp(T_prev[ndx][0]));
        lhs[ndx-1][ndx-1] = 4.0*dx/(6.0*dt)+2.0*VALUEk(T_prev[ndx][0])/\
                                        (rho*dx*VALUECp(T_prev[ndx][0]));
        invers(ndx,lhs,lhs_inv);
        mult_mat(ndx,ndx,ndx,1,lhs_inv,rhs,T_pres);

/*      HEAT TRANSFER COEFFICIENT       */

        dum   = dx/(6.0*dt)*(2.0*Tc+T_pres[0][0])+VALUEk(T_prev[0][0])/\
                (rho*dx*VALUECp(T_prev[0][0]))*(Tc-T_pres[0][0]);
        dum1 = dx/(6.0*dt)*(2.0*T_prev[0][0]+T_prev[1][0]);
        h = -(dum-dum1)*rho*VALUECp(T_prev[0][0])/(Tc-Tw);
        fprintf(ofp,"%f\t%lf\t%lf\t%.10lf\n",ndt*dt,Tc,Th,h);

        ndt++;
        T_prev[0][0] = Tc; T_prev[nodxs-1][0] = Th;
        for (i = 0; i <= ndx-1; i++)
        T_prev[i+1][0] = T_pres[i][0];
        } while (ndt <= nodts-1);

        fclose(ifp);
        fclose(ffp);
        fclose(ofp);
return 0;
}
double VALUECp(double T)
{
        double valueCp;
 extern int mater;

        switch (mater) {
        case 1:
        if (T < 200.0) valueCp = 0.29*T+464.25;
        else if (T < 250.0) valueCp = 0.23*T+476.25;
        else if (T < 300.0) valueCp = 0.61*T+380.25;
        else if (T < 350.0) valueCp = 0.23*T+494.25;
        else if (T < 400.0) valueCp = 0.45*T+428.75;
        else if (T < 500.0) valueCp = 0.536*T+394.0;
        else if (T < 600.0 ) valueCp = 0.768*T+266.4;
        else if (T < 700.0) valueCp = 0.57*T+385.1;
        else if (T < 750.0) valueCp = 1583;
        else if (T < 900.0) valueCp = -0.76*T+1213.0;
```

```c
        break;
        case 2:
        if (T < 100.0) valueCp = 0.052*(T-20.0)+384.93;
        else if (T < 200.0) valueCp = 0.1256*(T-100.0)+389.11;
        else if (T < 500.0) valueCp = 0.083*(T-200.0)+401.67;
        else if (T < 1000.0) valueCp = 0.092*(T-500.0)+426.77;
        break;
        case 3:
        valueCp = 0.385;  }

return (valueCp);
}
double VALUEk(double T)
{
        double valuek;
 extern int mater;

        switch (mater) {
        case 1:
        if (T < 200.0) valuek = 53.2 - 0.025 * T;
        else if (T < 300.0) valuek = 53.4 - 0.026 * T;
        else if (T < 400.0) valuek = 56.7 - 0.037 * T;
        else if (T < 500.0) valuek = 57.1 -0.038 * T;
        else if (T < 600.0) valuek = 59.1 -0.042 * T;
        else if (T < 700.0) valuek = 56.7 -0.038 * T;
        else if (T < 800.0) valuek = 67.9 - 0.054 * T;
        else if (T < 1000.0) valuek = 16.3 + 0.0105 * T;
        break;
        case 2:
        valuek = 338.0;
        case 3:
        if (T == 100.0) valuek = 128.1;
        else if (T == 200.0) valuek = 143.9;
        else if (T == 300.0) valuek = 147.1;
        else if (T == 400.0) valuek = 147.1;
        else
        valuek = 111.638 + 0.207103*T-(28.1967e-05)*T*T-\
                                   (4.42963e-08)*T*T*T;
        break; }
return (valuek);
}
void nrerror(char *error_text)
{
        printf("ERROR : %s\n",error_text);
        printf("...now exiting to system...");
        exit(1);
}
```

118404